

Peter B. Stathopoulos
Mitsuhiro Ikura

Structurally delineating stromal interaction molecules as the endoplasmic reticulum calcium sensors and regulators of calcium release-activated calcium entry

Authors' address

Peter B. Stathopoulos¹, Mitsuhiro Ikura¹

¹Division of Signaling Biology and Department of Medical Biophysics, Ontario Cancer Institute and University of Toronto, Toronto, ON, Canada.

Correspondence to:

Mitsuhiro Ikura

Division of Signaling Biology and Department of Medical Biophysics

Ontario Cancer Institute and University of Toronto

Toronto Medical Discovery Tower, MaRS Centre

101 College Street

Toronto, ON, Canada M5G 1L7

Tel.: +1 416 581 7550

Fax: +1 416 581 7549

e-mail: mikura@uhnres.utoronto.ca

Acknowledgements

This work was possible through a Canadian Institutes of Health Research operating grant (to M. I.), Canadian Foundation for Innovation grant (to M. I.) for an 800 MHz NMR spectrometer at the Toronto Medical Discovery Tower, and Natural Sciences and Engineering Research Council of Canada and Ontario Cancer Institute Knudson fellowships (to P. B. S.). M. I. holds the Canada Research Chair in Cancer Structural Biology.

Summary: The endoplasmic reticulum (ER) lumen stores a crucial source of calcium (Ca^{2+}) maintained orders of magnitude higher than the cytosol for the activation of a plethora of cellular responses transmitted in health and disease by a mutually efficient and communicative exchange of Ca^{2+} between compartments. A coordination of the Ca^{2+} signal is evident in the development of Ca^{2+} release-activated Ca^{2+} (CRAC) entry, vital to lymphocyte activation and replenishing of the ER Ca^{2+} stores, where modest decreases in ER luminal Ca^{2+} induce sustained increases in cytosolic Ca^{2+} sourced from steadfast extracellular Ca^{2+} supplies. While protein sensors that transduce Ca^{2+} signals in the cytosol such as calmodulin are succinctly understood, comparative data on the ER luminal Ca^{2+} sensors is only recently coming to light with the discovery that stromal interaction molecules (STIMs) sense variations in ER stored Ca^{2+} levels in the functional regulation of plasma membrane Orai proteins, the major component of CRAC channel pores. Drawing from data on the role of STIMs in the modulation of CRAC entry, this review illustrates the structural features that delimit the functional characteristics of ER Ca^{2+} sensors relative to well known cytoplasmic Ca^{2+} sensors.

Keywords: stromal interaction molecule, store-operated calcium entry, calcium release-activated calcium, EF-hand, sterile α -motif, calcium sensor

Introduction

Calcium (Ca^{2+}) is a vital messenger in all eukaryotic cells, differentially regulating diverse cellular phenomena via spatiotemporal partitioning of Ca^{2+} levels (1). External stimuli provoke alterations in basal intracellular Ca^{2+} concentrations $[\text{Ca}^{2+}]_i$, directly or indirectly effecting proteins that regulate, for example, exocytosis, contraction, metabolism, transcription, fertilization, proliferation, vision, memory, and the immune response (2). Eukaryotic cells maintain low resting free Ca^{2+} concentrations in the cytosol (i.e. sub- μM) so that only small fluctuations in local $[\text{Ca}^{2+}]_i$ levels (i.e. 10^{-7} – 10^{-6} M) can yield a signaling effect; moreover, the evolution of the Ca^{2+} signal in this regard precludes the large energetic cost associated with shifting high local ion concentrations and

Immunological Reviews 2009

Vol. 231: 113–131

Printed in Singapore. All rights reserved

© 2009 John Wiley & Sons A/S

Immunological Reviews

0105-2896

overcomes the poor solubility of cytoplasmic Ca^{2+} -phosphate salts at elevated Ca^{2+} levels (3). Ca^{2+} -binding proteins acting on various enzymes and downstream effectors decode, potentiate, and transduce the Ca^{2+} signals, playing vital negative and positive feedback roles in Ca^{2+} transport and ultimately enabling cells to generate rapid changes in local Ca^{2+} levels in phenomena known as spikes and waves (2).

The endoplasmic reticulum (ER) compartmentalizes an internal store of Ca^{2+} imperative to sourcing transient cytosolic $[\text{Ca}^{2+}]_i$ changes. The ER lumen maintains Ca^{2+} levels that are at least two orders of magnitude higher than the cytoplasm (Fig. 1); this steep pitch in concentration is essential for rapid signaling to the cytosol at a low energetic cost. A cytosolic transient which results from diminishing a high fraction of the Ca^{2+} store would be detrimental, as numerous fundamental Ca^{2+} -dependent processes are implemented within the ER lumen (i.e. protein folding, degradation, chaperonal activity,

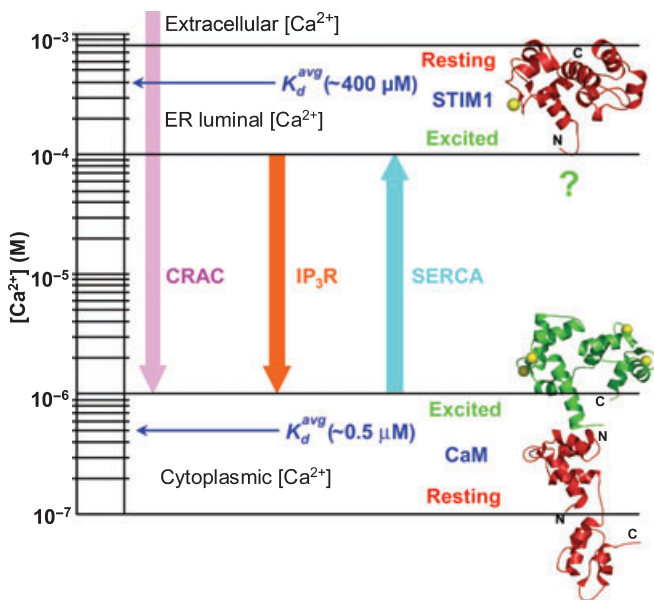


Fig. 1. Ca^{2+} interchange and sensing in SOCE/CRAC entry. The cytoplasm functions at Ca^{2+} concentrations in the range of the affinity estimates for the four binding sites of CaM. At low Ca^{2+} , CaM is in a 'resting' state characterized by the absence of intermolecular target interactions. At high cytoplasmic Ca^{2+} , the binding sites are saturated, and the EF-hands are in the 'open' conformation suitable for target interaction. The ER lumen operates at Ca^{2+} levels at least two orders of magnitude higher than the cytoplasm. The Ca^{2+} affinity of known ER sensors is in the same range as estimates for luminal Ca^{2+} concentrations. However, the ER sensor is dormant with 'open' EF-hand intramolecular interactions at saturating Ca^{2+} levels, and in the active 'excited' state upon luminal depletion. Ca^{2+} moves from the lumen to the cytoplasm via IP_3 receptors (IP_3R) (orange arrow); however, molecular signaling as a result of sensing in the lumen triggers Ca^{2+} release into the cytoplasm from the extracellular space via CRAC channels (purple arrow). Ultimately, sarcoplasmic/ER Ca^{2+} -ATPase (SERCA) pumps refill the lumen from cytoplasmic Ca^{2+} (cyan arrow). K_d^{avg} , average of the range of Ca^{2+} dissociation constants.

vesicle trafficking, lipid, and steroid biosynthesis) (4). Although the ER occupies a large space within cells providing a significant transient source of Ca^{2+} , a more steadfast supply of the signaling ion is available to eukaryotes in the extracellular medium, where Ca^{2+} levels are maintained several orders of magnitude higher than the cytosol (i.e. approximately 1–2 mM) (Fig. 1). Synchronization of ER luminal Ca^{2+} efflux with extracellular Ca^{2+} influx into the cytoplasm is essential, as unrelentingly high $[\text{Ca}^{2+}]_i$ is cytotoxic and can lead to apoptosis and necrosis.

The Ca^{2+} flux protein machinery consisting of ion channels, pumps, exchangers, buffers, as well as sensors coordinate highly localized Ca^{2+} signals with contributions from every cellular compartment (1, 2). An example of harmonization between Ca^{2+} signals originating from both the ER luminal store and extracellular space is store-operated Ca^{2+} entry (SOCE). Eukaryotes have evolved SOCE, also known as capacitive Ca^{2+} entry, as a principal Ca^{2+} entry pathway for achieving a prolonged elevation of cytoplasmic $[\text{Ca}^{2+}]_i$. Although the model for this evolutionarily conserved signaling process was proposed almost 25 years ago (5), the molecular flux components were only recently identified and characterized. SOCE is the process whereby the ER luminal Ca^{2+} store depletion leads to the formation and opening of highly selective plasma membrane (PM) Ca^{2+} channels that facilitate a sustained increase in $[\text{Ca}^{2+}]_i$; this prolonged increase in cytosolic Ca^{2+} is crucial for stimulating a cellular response (e.g. transcription activation) and for replenishing the ER stores (6).

In lymphocytes, SOCE through PM Ca^{2+} release-activated Ca^{2+} (CRAC) channels is the principal means of increasing cytosolic Ca^{2+} levels. In the absence of sustained Ca^{2+} influx through CRAC channels, lymphocyte activation, proliferation, and other effector functions are severely compromised, leading to rare but very intrusive immunodeficiency diseases (7–10). Overall, Ca^{2+} signaling in lymphocytes is well defined. T-cell receptor or G-protein-coupled receptor stimulation signals phospholipase-dependent catalysis of phosphatidylinositol 1,4-bisphosphate to 1,4,5-trisphosphate (IP_3). IP_3 is a diffusible messenger that binds to the IP_3 receptor located on the ER membrane, promoting Ca^{2+} efflux from the ER lumen. SOCE is initiated and CRAC entry ensues, providing the principal source of cytoplasmic Ca^{2+} for cytokine secretion and proliferation critical to the immune response (11).

Transient receptor potential (TRP) channels have long been proposed to be components of CRAC entry (12, 13); however, the TRP link is tumultuous due to the inability of TRP knock-down to affect SOCE/CRAC entry (12, 14) and other more recent conflicting data (*vide infra*). In 2005, stromal interaction

molecule-1 (STIM1) was identified by two independent inhibiting ribonucleic acid (RNAi) studies as an ER luminal protein that senses Ca^{2+} depletion and regulates the opening of PM Ca^{2+} channels (15–17), the first such acknowledged ER Ca^{2+} -dependent sensor. In 2006, an additional major component of the PM Ca^{2+} channel was identified in Orai1 (or CRACM1) by pedigree analysis of inheritable severe combined immunodeficiency patients and RNAi studies (10, 18, 19); the Orai1 protein has since been confirmed as the major SOCE Ca^{2+} channel pore subunit on the PM (20–22). To fully appreciate the unique function conferred by STIM ER Ca^{2+} sensors, an overview of the structure and function relationship of model intracellular Ca^{2+} sensors is provided.

Paradigm of intracellular Ca^{2+} sensing

Intracellular Ca^{2+} sensors are proteins that undergo a conformational response to the binding or dissociation of the Ca^{2+} ion, ultimately mediating a specific cellular function through a biomolecular interaction (23). The function of sensors is different from protein buffers, which bind or release Ca^{2+} to preserve or fine-tune local Ca^{2+} levels, and unlike pumps and exchangers, which shuttle Ca^{2+} between compartments against a concentration gradient. Most intracellular Ca^{2+} sensor proteins employ a well-characterized Ca^{2+} -binding motif termed the EF-hand, first elucidated at the atomic level in the parvalbumin crystal structure (24). The EF-hand motif consists of a helix-loop-helix architecture with a 12 residue interhelical loop containing several consensus amino acids for coordination of a single Ca^{2+} ion. Typically, a pair of EF-hand motifs constitutes a single structural unit, generating Ca^{2+} binding cooperativity, increasing structural stability, and augmenting Ca^{2+} sensitivity (25–27). The archetypal Ca^{2+} sensor crucial for various signaling processes is calmodulin (CaM), which maintains a very high sequence conservation from roundworms to humans (28). CaM (148 residues) encodes two EF-hand domains (i.e. four total EF-hand motifs) that are linked through a central flexible linker; moreover, all four binding loops coordinate Ca^{2+} with high affinity (i.e. K_d approximately 0.1–1 μM) and cooperativity (29). While CaM and many other Ca^{2+} sensor proteins (e.g., DREAM and Ca^{2+} -binding protein 1) encode four motifs, several sensors encode only a pair (e.g. S100 proteins and nucleobindin); these aforementioned Ca^{2+} sensor proteins all function in the cytoplasm or nucleus. However, in some instances only a single EF-hand motif is detectable by sequence analysis (*vide infra*).

While many Ca^{2+} sensors have genetically evolved polymorphic isoforms for recognition of different targets in

sensing function, CaM is structurally capable of adapting to many binding partners (28). Two structural characteristics in CaM promote this promiscuity: first, a long central helix connecting the two EF-hand domains (i.e. EF-hand pairs) has a flexible portion (residues 78–81) that can be dramatically bent, allowing each domain to change independently in the accommodation of a target, and second, the hydrophobic cleft formed by each domain is rich in Met amino acids that confer a local litheness for intimate interaction with different hydrophobic residues (25, 28, 30). The list of CaM binding partners is too great to review here (i.e. over 300 targets) (31); however, many proteins important in T-cell activation are regulated via heterotypic CaM interactions in the cytosol such as the calcineurin phosphatase (32), the ER-membrane anchored IP_3 receptor (33), CaM kinase II, and CaM kinase IV (34). CaM also has been shown to interact with the cytosolic portion of both STIM1 and STIM2 in cell culture and *in vitro* (35, 36).

CaM is an effective cytosolic Ca^{2+} sensor, as it can structurally and functionally respond to (i.e. sense) changes in the range of signals generated by Ca^{2+} spikes, waves, and oscillations within the cytoplasm. To achieve this sensitivity, CaM binds Ca^{2+} with high affinity (see before) and cooperativity, so that the liganding of one Ca^{2+} ion increases the affinity of the paired (i.e. backbone hydrogen bonded) loop for the next Ca^{2+} ion; the sharp Ca^{2+} response facilitated by cooperativity of Ca^{2+} binding confers an effective on–off molecular switch function for CaM (Fig. 1). The low cytosolic Ca^{2+} levels define the need for intricate Ca^{2+} binding dynamics in cytosolic sensor proteins. How do compartmentalized Ca^{2+} sensors function when Ca^{2+} levels are maintained orders of magnitude higher than the cytosol? STIM1, the recently discovered Ca^{2+} sensor of the ER and essential activator SOCE, has shed considerable light on the sensing mechanism within the ER lumen. The focus of this review is on the structural and functional characteristics of STIM molecules with respect to CRAC channel activation in response to Ca^{2+} depletion within the ER lumen. The available data define an archetypal ER Ca^{2+} sensor with some similarities but more important distinctions compared with cytosolic sensors (i.e. CaM) that divide this important class of Ca^{2+} -binding proteins.

STIMs as ER-specific Ca^{2+} sensors

Sequence-based putative STIM domains

Human STIM1 is expressed as a 685 amino acid, type-I transmembrane protein with the C-terminal domains oriented within the cytoplasm (Fig. 2A). While a fraction of STIM1 has

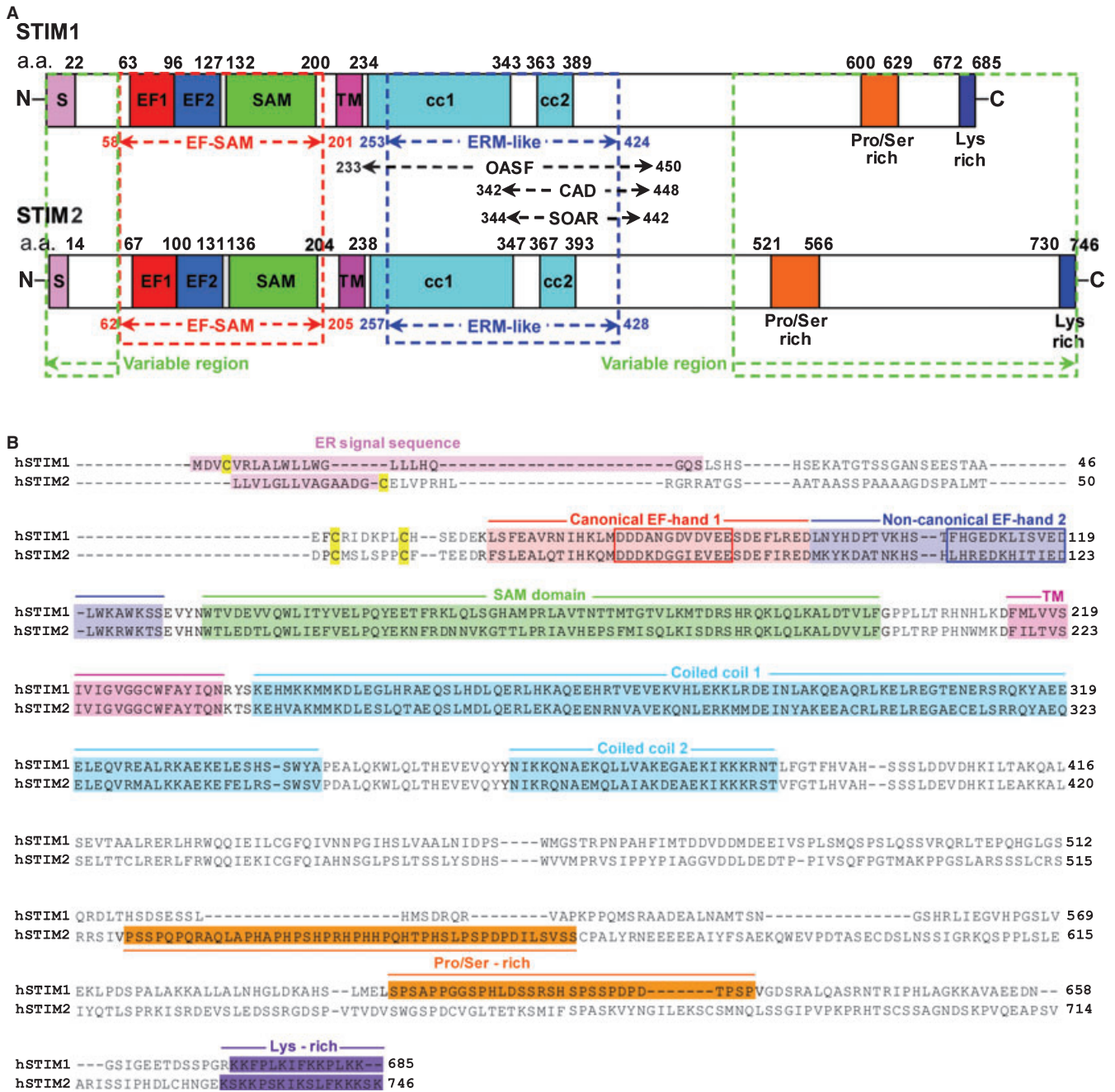


Fig. 2. Comparative domain architecture of the STIMs. (A) Domain architecture of human STIM1 and STIM2. The luminal regions of STIMs contain highly conserved EF-hand and SAM domains (red broken box). The molecules are largely variable in a region proximal to the EF-SAM domain towards the N-terminus (green broken box). The cytosolic portion contains two coiled-coil domains encoded through an ERM-like domain (blue broken box). This highly conserved ERM-like region contains the OASF/CAD/SOAR regions functionally recognized as the activation domains of Orail. Human STIMs also encode conserved Pro/Ser-rich and Lys-rich stretches within the otherwise variable C-termini (green broken box). (B) Sequence alignments of human STIM1 and STIM2. STIM1 (accession: NM_003156) and STIM2 (accession: NM_020860) sequences were aligned in ClustalW (118). Residues exhibiting high conservation are shaded the corresponding color from Fig. 2A. All luminal cysteines are shaded yellow. Identified and putative regional boundaries are indicated above each aligned stretch of amino acids. The canonical EF-hand binding loop is bounded with a red box and the non-canonical loop is bounded by with a blue box. N, amino-terminus; S, ER signal peptide; EF1, canonical EF-hand 1; EF2, non-canonical EF-hand 2; TM, transmembrane region; cc1, coiled coil-1; cc2, coiled-coil-2; ERM, ezrin-radixin-moesin homology region; C, carboxy-terminus (adapted from 69, 86).

been detected on the PM, most is localized on the ER membrane positioning the N-terminal domains in the extracellular space or ER lumen (15, 17, 37, 38). An ER localization signal,

a single EF-hand motif and a sterile α -motif (SAM) domain have been identified within the N-terminal sequence of the protein (39, 40). These N-terminal domains are implicated in

Ca²⁺-sensing (*vide infra*). Post-translational modifications have been characterized at specific Asn131 and Asn171 residues, residing in the SAM domain, and have been implicated in targeting STIM1 to the PM (41, 42). The N-terminal domains are predicted to be separated from the C-terminal domains by a single transmembrane-spanning segment (39). There are two sequence-presumed coiled-coil regions within the cytoplasmic domains of STIM1; moreover, both these domains fall within an ezrin–radixin–moesin (ERM)-like domain. Other features of interest on the C-terminal side of the protein include a Lys-rich domain and a Pro/Ser-rich region; phosphorylation occurs at several Ser and Thr sites within the Pro/Ser-rich region (37).

Mammals express a second isoform, STIM2, which is encoded with high sequence similarity (i.e. > 65%) to STIM1 (Fig. 2A, B). The greatest variation between the human homologs occurs after the coiled-coil domains towards the C-terminus (40, 43); however, there is also noted variability at the N-terminal distal end of the proteins. The distribution of STIM2 seems to be limited to the ER membrane, despite the conserved Asn131 glycosylation site (i.e. Asn135 in STIM2); this restricted localization may be due to a consensus ER-retention signal in STIM2 (43). The most conserved domains among invertebrate and vertebrate phylogeny (i.e. from roundworms to flies to humans) are the EF-hand, SAM, coiled-coil, and ERM-like regions (40).

Cell biology studies have established that ER luminal Ca²⁺ depletion results in a drastic redistribution of STIM1 from homogeneous dispersion on the ER membrane to specific cluster sites at ER–PM junctions (16, 17). The movement of STIM1 to the discrete ER–PM cluster sites facilitates the recruitment of the Orai1 component of the CRAC channel to the same junctions, requisite for the sustained SOCE/CRAC entry (44–47). Co-overexpression of these proteins radically enhances CRAC current (i.e. the inward rectifying current–voltage relationship generated by the cytoplasmic influx of divalent Ca²⁺ ions through PM CRAC channels) intimating that both STIM1 and Orai1 are molecular components integral to the formation SOCE/CRAC entry (18, 48–50).

How does the Ca²⁺ sensing initiate STIM1 targeting to ER–PM junctions inducing the subsequent opening of the Ca²⁺ channel pore? Cell biology experiments have improved the understanding of the role that the most conserved STIM1 cytoplasmic regions play in STIM1 targeting to sites in close apposition to the PM and activation of Orai1 (51–54) (*vide infra*). However, interest in defining STIM1 as the long sought after Ca²⁺ sensor of the ER lumen existed in earlier studies that linked STIM1 with SOCE/CRAC entry. It is presently established

that the machinery required for the sensitivity to Ca²⁺ is encoded within the N-terminal, ER lumen-oriented domains of STIM1. Cell studies demonstrate that mutation of vital canonical Ca²⁺ liganding residues within the binding loop of the EF-hand motif results in constitutive puncta (i.e. oligomerization of STIM1 and clustering at ER–PM junctions with Orai1) formation and activation of SOCE/CRAC entry, presumably due to the inability of the loop to coordinate Ca²⁺ (16, 17, 38, 49). Furthermore, deletion of the SAM domain produces a STIM1 variant insensitive to Ca²⁺ and thus incapable of forming inducible puncta (51). Oligomerization of STIM1 due to ER-stored Ca²⁺ depletion is a key sensory event in the activation of CRAC channels and occurs prior to accretion of STIM1 at ER–PM junctions (53). The significance of this preliminary oligomerization step was fully appreciated in an elegant study that replaced the EF-hand together with the SAM domain, hereafter referred to as EF–SAM, with the FK506- and rapamycin-binding protein (FKBP12) or FKBP rapamycin-binding (FRB) domain of mammalian target of rapamycin. FKBP12 and FRB served as Ca²⁺-independent protein interaction domains, inducible by rapamycin or analogs thereof; moreover, SOCE/CRAC entry was induced irrespective of ER luminal Ca²⁺ levels by treatment with rapamycin in cells expressing the STIM1–FRB/FKBP12 fusions (55). The study (55) demonstrated the crucial role for the oligomerization sensory function endowed by EF–SAM within STIM proteins in triggering the arrangement of an active STIM1–Orai1 CRAC complex at ER–PM junctions.

Characterization of EF–SAM

Biochemical and biophysical features of STIM1 EF–SAM

The importance of the cell biological studies to the elucidation of STIM sensory function cannot be understated; however, data linking the primary sequence to the in-cell functional observations are important for defining the requisite machinery and mechanism of ER luminal Ca²⁺ sensing associated with activation of SOCE/CRAC entry. To bridge this gap, the Ca²⁺-sensing region of STIM1 was examined using higher resolution biophysical and biochemical tools. As the most conserved N-terminal region among STIM isoforms is EF–SAM, experimental focus in this regard was on a recombinant protein expressed in *Escherichia coli* that encompassed residues 58–201 of STIM1 (Fig. 2A, B). Because of the high sequence conservation from lower to upper eukaryotes (40, 56), the fundamental sensing characteristics of STIM1 EF–SAM are likely to be representative of all STIM isoforms, with specific distinctions defined by subtle changes in primary sequence and three-dimensional (3D) atomic structures.

The STIM1 EF-SAM recombinant protein is well folded in the presence of relatively high concentrations of Ca^{2+} (i.e. 1–2 mM). The high level of α -helical secondary structure in the Ca^{2+} -loaded state, readily identifiable using far-ultra violet (UV) circular dichroism (CD), is consistent with primary amino acid prediction analyses (57). In the absence of Ca^{2+} , a marked structural contrast is observed for EF-SAM, which loses considerable α -helicity, unpredicted by sequence analysis. Backbone amide $^1\text{H}(\text{N})$ resonance dispersion in ^1H - ^{15}N HSQC correlation spectra measured by solution nuclear magnetic resonance (NMR) confirms the large conformational differences of EF-SAM in the presence and absence of Ca^{2+} , with Ca^{2+} -depleted protein solutions exhibiting much narrower $^1\text{H}(\text{N})$ dispersion of peaks. Size exclusion chromatography (SEC) with in-line multi-angle light scattering (MALS) shows that Ca^{2+} -loaded EF-SAM exists in a rigorously monomeric state, while Ca^{2+} -depleted STIM1 EF-SAM is in equilibrium between a dimer and higher order oligomers. The differences in quaternary structure are also identifiable in NMR ^1H - ^{15}N HSQC spectra, where Ca^{2+} -depleted $^1\text{H}(\text{N})$ peaks are appreciably broadened compared with those measured in the Ca^{2+} -loaded state (57).

ER luminal Ca^{2+} store refilling is an essential corollary of SOCE/CRAC entry (5, 6). In the absence of such a feedback mechanism, an enduring augmentation of cytosolic Ca^{2+} would lead to apoptotic or necrotic cell death (58). SOCE-dependent luminal store refilling and reversal of STIM1 puncta are essential for the inactivation of PM CRAC channels (47, 53, 59). Consistent with this notion, cells with unmitigated puncta due to expression of STIM1 with Ca^{2+} -binding mutations stain positive for an apoptotic marker (i.e. annexin-V) (17). The observation that *in vitro* STIM1 EF-SAM reversibly undergoes a monomer-to-oligomer transition in the presence and absence of Ca^{2+} , respectively, demonstrates the significance of the conserved luminal region within STIM molecules in controlling puncta formation and is fully consistent with *in-cell* observations (57). The Ca^{2+} -dependent structural transformations of EF-SAM imparts an initial attribute to the definition of an ER Ca^{2+} sensor.

The recombinant EF-SAM protein is useful for appraising the affinity of a sensor situated in an environment with elevated Ca^{2+} levels (i.e. the ER lumen). Radioactive $^{45}\text{Ca}^{2+}$ binding measurements directly confirm the ability of EF-SAM to bind Ca^{2+} ; moreover, the estimated binding affinity using the same assay is low compared with cytoplasmic sensors (i.e. K_d approximately 0.2–0.6 mM) (57). The stoichiometry of binding appears to be approximately 1, consistent with encoding a single EF-hand motif. A single downfield shifted

$^1\text{H}(\text{N})$ resonance assigned to Gly81 is observed in ^1H - ^{15}N correlation spectra, implying that Ca^{2+} coordination occurs in a canonical manner within the binding loop (60, 61). Indirect binding assays using Ca^{2+} -dependent structural changes (i.e. intrinsic fluorescence and far-UV CD) as a probe to the fractional saturation of the protein confirm the low affinity and imply that binding is somewhat temperature dependent, with higher affinities observed at lower temperatures (57). *In-cell* studies have estimated the ER Ca^{2+} concentration where STIM1 puncta formation is half maximal to be approximately 0.2 mM, consistent with the binding affinity measurements on EF-SAM (55, 62). The binding experiments on EF-SAM show a steep cooperativity, even though only a single Ca^{2+} ion appears to be coordinated in this STIM1 region. As Ca^{2+} -depleted STIM1 EF-SAM exists as a dimer and oligomer, the apparent cooperativity may reflect the effect of coordination in one site on the affinity of another site within the same protein complex. Alternatively, the observed cooperativity may be due to restructuring of EF-SAM as a function of Ca^{2+} concentration, as protein folding is inherently cooperative (63). The cooperativity observed in Ca^{2+} binding to EF-SAM is different than the cooperativity observed for full-length STIM1 puncta formation; the *in-cell* cooperativity indicates that pre-oligomerized STIM1 accretes at ER-PM junctions rather than monomeric STIM1 (55). Overall, the estimated Ca^{2+} -binding affinity of STIM1 EF-SAM is reconcilable with the high Ca^{2+} levels of the ER lumen (Fig. 1) and confers an additional attribute in the definition of an ER Ca^{2+} sensor.

Coordination of Ca^{2+} drastically enhances the stability of STIM1 EF-SAM, increasing the melting temperature (i.e. temperature where the fraction of unfolded macromolecules = 0.5) by approximately 26 °C. The heat capacity change upon unfolding is considerably higher for the Ca^{2+} -loaded state compared with the -depleted state, reflecting a greater change in solvent accessible surface area and consistent with the steeper denaturant dependence observed for the holo protein in urea unfolding experiments (57, 64). The thermodynamic analyses offer insight into the solvent accessibility differences of EF-SAM in the presence and absence of Ca^{2+} , where the apo protein exists in a less compact and more solvent accessible state. 1-Anilino-8-naphthalene-sulfonate (ANS) extrinsic fluorescent experiments demonstrate that the expanded apo EF-SAM structure contains greater solvent accessible non-polar character than the Ca^{2+} -loaded protein (57, 65). Thus, the sensory function of STIM molecules may be additionally delineated by sizeable changes in the stability-defining physicochemical parameters that accompany the binding and release of Ca^{2+} .

Biochemical and biophysical features of STIM2 EF-SAM

Delineating the sensory function of human STIM2 is more challenging than STIM1, due to capricious in-cell observations. Preliminary reports linking STIM1 to SOCE/CRAC entry are contradictory in terms of the significance of STIM2 in mediating the same process (15, 16). Subsequent studies suggested that STIM2 is an inhibitor of STIM1-mediated SOCE/CRAC entry in various cell types (48, 49, 66). A follow-up investigation qualified previous results in suggesting that STIM2 activates Orai1 channels by ER Ca^{2+} store-dependent and -independent modes of action and that CaM as well as G418 (i.e. an aminoglycoside antibiotic) inhibit STIM2-mediated SOCE/CRAC entry (35). Additionally, an ER Ca^{2+} store-dependent role for STIM2 in the maintenance of basal Ca^{2+} levels is described (62), and a crucial role for STIM2 in SOCE/CRAC entry is implied from data showing that T-cells have markedly decreased cytokine production and transcriptional factor (i.e. nuclear factor of activated T-cells) translocation, even though SOCE/CRAC entry is not as impaired in cells lacking STIM2 compared with STIM1 (67).

Exchanging a portion of the STIM1 canonical EF-hand loop (i.e. residues 79–82) with the sequence-aligned residues from STIM2 increases basal Ca^{2+} levels as a function of protein expression in mammalian cells above that observed for wild-type STIM2; however, substituting STIM1 residues into STIM2 does not induce STIM1-like behavior from mutant STIM2 (62). These data not only imply a vital role for the EF-hand loops in influencing the functional discrepancies between STIM isoforms but also suggest that other domains are involved in fashioning the full sensory nuances of the proteins. Experiments that characterize the biophysical and biochemical properties of recombinant STIM2 EF-SAM (i.e. encompassing residues 62–205) (Fig. 2A) offer additional data on the functional divergence between STIM proteins. Estimation of a dissociation constant for STIM2 EF-SAM using the same $^{45}\text{Ca}^{2+}$ experimental setup as STIM1 is not possible due to a large variability in the saturated radioactivity of the protein; moreover, the larger baseline error for STIM2 compared with STIM1 EF-SAM implies a lower affinity for STIM2 on a qualitative level. However, STIM2 EF-SAM dissociation constants indirectly estimated from far-UV CD demonstrate that the Ca^{2+} affinity of STIM2 EF-SAM are of same magnitude as observed for STIM1 (i.e. sub-mM) (68). A single downfield shifted $^1\text{H}(\text{N})$ resonance assigned to gly86 is observed in the $^1\text{H}-^{15}\text{N}$ HSQC spectra, indicative of canonical Ca^{2+} coordination within the putative STIM2 EF-SAM loop (60, 61). In-cell studies show that the concentration of Ca^{2+} within the ER

lumen where redistribution of STIM2 into puncta is half maximal is approximately 0.4 mM, in good agreement with affinity estimates using recombinant EF-SAM (i.e. K_d approximately 0.5 mM) (62, 68). Thus, low Ca^{2+} affinity that is in-line with ER luminal Ca^{2+} levels is a defining hallmark of ER Ca^{2+} sensors (Fig. 1).

Despite the rather similar Ca^{2+} affinities, STIM2 EF-SAM is much more stable than the STIM1 counterpart in both the Ca^{2+} -loaded and -depleted states. The far-UV CD spectrum demonstrates high α -helicity for holo STIM2 EF-SAM, as observed for STIM1; however, in the Ca^{2+} -depleted state, STIM2 EF-SAM retains most of the helicity at low temperatures, in contrast to STIM1 EF-SAM, which loses much of this secondary structure. Thermal denaturation of STIM2 EF-SAM is in-line with the gross structural data, in that the melting temperature of apo and holo STIM2 EF-SAM is approximately 15 °C and 5 °C higher, respectively, compared with STIM1. The considerably enhanced stability of the apo state translates into an ability of Ca^{2+} -depleted STIM2 EF-SAM to maintain a monomeric albeit less-compact conformation at low temperatures, deduced from SEC elution profiles. Nonetheless, destabilization of apo STIM2 EF-SAM by increasing the temperature induces oligomerization of the recombinant protein, monitored by $^1\text{H}-^{15}\text{N}$ HSQC spectra, which have severely broadened peaks, and SEC, which shows the protein largely in the void volume [i.e. in S200 Superdex columns (GE Healthcare, Baie d'Urfe, Canada)]. The oligomerization of apo STIM2 EF-SAM is concentration dependent, with higher protein concentrations more readily oligomerizing; moreover, oligomerization is coupled with a loss in α -helicity, monitored by far-UV CD (68). The EF-SAM data advocate a Ca^{2+} -depletion-dependent sensory definition for STIM proteins that involves homotypic protein-protein interactions; both STIM1 and STIM2 EF-SAM have an inherent ability to homotypically interact.

Atomic resolution structure of STIM1 EF-SAM

Structural topology of Ca^{2+} -loaded STIM1 EF-SAM

Atomic level structural detail of STIM proteins is largely absent. Three-dimensional structural information combined with the in-cell functional and in vitro biophysical studies are imperative to comprehensively understand the molecular forces that govern Ca^{2+} sensing and activation of SOCE/CRAC entry. Available structural information is limited to the recombinant EF-SAM protein of STIM1. The high quality solution data from conventional NMR experiments for Ca^{2+} -loaded STIM1 EF-SAM offers a means to the extensive structural

analysis of the protein. The nuclear Overhauser effect (NOE)-based EF-SAM structural ensemble shows this region folds into a single compact tertiary structure consisting of 10 α -helices and two short anti-parallel β -strands (Fig. 3). The high helical content is fully consistent with far-UV CD and primary sequence analyses, while the single cooperative fold of the EF-hand together with the SAM domain is coherent with fitted two-state folding thermodynamics (57, 69).

'Hidden' structural components

The sequence-based canonical EF-hand motif is readily identified in the 3D structure, with the $\alpha 1$ - $\beta 1$ - $\alpha 2$ components making up the standard helix-loop-helix motif. The atomic structure brings to light a second helix-loop-helix motif in the $\alpha 3$ - $\beta 2$ - $\alpha 4$ EF-hand not recognized in sequence-based structural predictions. The loop of the non-canonical EF-hand is unable to form the tight turn required for Ca^{2+} coordination (70–72), but rather, prominently orients the carbonyl oxygen and amide hydrogen atoms of Ile115 for direct hydrogen-bonding with the amide hydrogen and carbonyl oxygen atoms of Val83 positioned in the canonical EF-hand loop; moreover, this hydrogen-bond configuration mutually stabilizes the EF-hand pair through the creation of a small anti-parallel β -sheet within EF-SAM (Fig. 3), as observed for other EF-hand-encoding proteins (73). A short helix, also unidentified by primary sequence analyses, links the EF-hand pair with the residues of the SAM domain. The SAM domain adopts a five-helix bundle ($\alpha 6$ - $\alpha 7$ - $\alpha 8$ - $\alpha 9$ - $\alpha 10$) that has been well characterized in other SAM domains (74–76). In addition to the cluster of hydrophobic residues within the SAM bundle

core (i.e. at the interface of the five helices) observed with other SAM domains, the STIM1 domain atypically arranges additional non-polar residues at the face opposite to that core on $\alpha 10$, directly adjacent to the EF-hand pair (Fig. 4).

The exterior surface of EF-SAM is primarily negatively charged at neutral pH. The electrostatic surface may play a role in the guidance of the divalent Ca^{2+} cation to the EF-hand binding loop. Residues from both the canonical and the non-canonical EF-hand contribute to the arrangement of a highly negative potential adjacent to the Ca^{2+} liganding site. EF-hand residues forming the electrostatic surface include Asp77, Asp78, Asp82, Asp84, Glu86, Glu87, Asp89, Glu90, Glu94, Asp95, Glu111, Asp112, Glu118, and Glu118 (69). The SAM surface also contributes anionic charges in the extension of the negative potential to the SAM side of the protein with Glu135, Glu136, and Asp196 residues (69). The predominantly anionic potential of EF-SAM contributes to the aberrant mobility of STIM in electrophoretic experiments (57, 69). However, it is important to note that several cationic amino acids also cluster on the SAM domain forming a prominent positive patch (i.e. Lys180, Arg184, Arg187, Lys189, Lys193), which may afford a binding site for oppositely charged nucleic acids (77, 78) or the surface of membrane lipids (79), as seen with other SAM domains.

Numerous structural homologs are found for both the EF-hand and the SAM domains encoded by STIM1. The most analogous structure for the EF-hand pair is the C-terminal domain of bovine Ca^{2+} -bound CaM with a backbone root mean square deviation (rmsd) of 3.2 Å (Fig. 5). The interhelical angles within the first EF-hand motifs of C-terminal CaM and STIM1 are nearly identical (i.e. approximately 80° versus

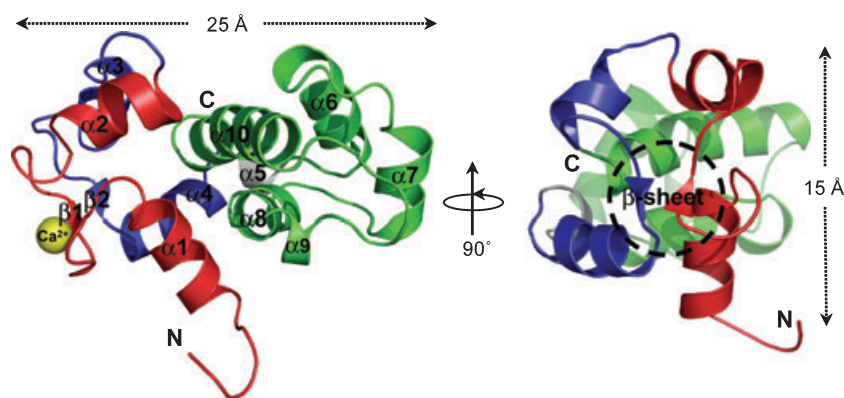


Fig. 3. Atomic 3D structure of STIM1 EF-SAM. Ca^{2+} -loaded EF-SAM folds into a compact entity consisting of ten α -helices and two anti-parallel β -strands. The canonical EF-hand (red backbone) coordinates the single Ca^{2+} ion (yellow sphere). The non-canonical EF-hand (blue backbone) stabilizes the canonical loop through backbone carbonyl and amide hydrogen-bonding. A short helix (grey backbone) sequentially links the EF-hand and SAM domains. The SAM domain (green backbone) folds into a five-helix bundle. For clarity, the small anti-parallel β -sheet is illustrated after a 90° rotation about the y-axis. Ribbons and arrowheads represent α -helix and β -strand secondary structures, respectively. Coloring is consistent with Fig. 2A. (pdbID: 2k60.pdb). Adapted from (69).

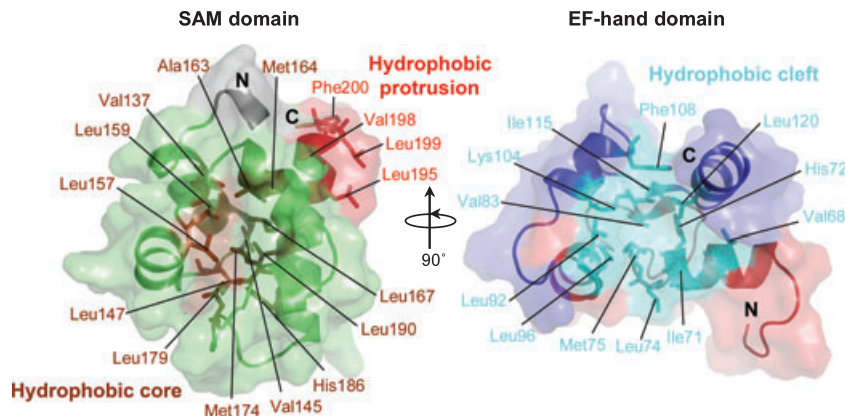


Fig. 4. Hydrophobic interactions within EF-SAM. The folded SAM domain contains a hydrophobic core formed by non-polar residues (brown sticks) contributed from each of the five helices (i.e., $\alpha 6$ – $\alpha 7$ – $\alpha 8$ – $\alpha 9$ – $\alpha 10$). A second hydrophobic patch created exclusively by $\alpha 10$ residues (red sticks) is buried on the opposite face of the domain via intimate packing with a large cleft formed by non-polar residues (cyan sticks) from the EF-hand domain. For clarity, the SAM and EF-hand domains are shown in the absence of the complementary binding domain with a 90° rotation about the y-axis. Coloring is consistent with Fig. 2A. (pdbID: 2k60.pdb). Adapted from (69).

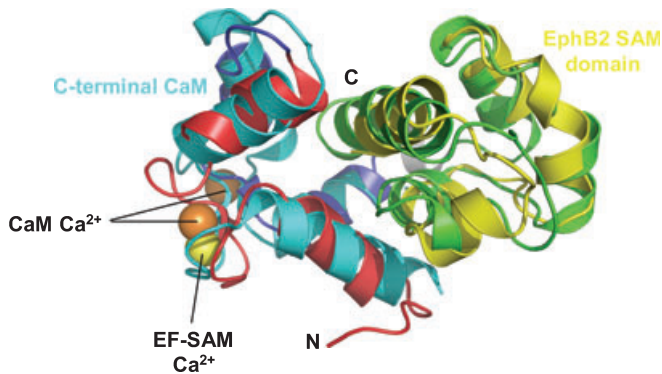


Fig. 5. EF-SAM structural homologs. The C-terminal EF-hand domain of Ca^{2+} -loaded bovine CaM (pdbID: 1prw.pdb; cyan backbone) is the nearest structural homolog to the EF-hand pair of STIM1 (red and blue backbone). The SAM domain of the EphB2 tyrosine kinase receptor (pdbID: 1b4f.pdb; yellow backbone) most closely resembles the SAM domain of STIM1 (green backbone). Structural homologs were searched for using the DALI server (119). Ca^{2+} ions coordinated by CaM and EF-SAM are shown as orange and yellow spheres, respectively.

82°, respectively), while the angles of second EF-hand pair are less similar but also in a noticeably ‘open’ conformation. ‘Open’ EF-hands, defined by interhelical angles of greater than approximately 70°, are a hallmark of many Ca^{2+} -loaded EF-hands; moreover, the ‘open’ conformation exposes several non-polar residues for hydrophobically mediated biomolecular interactions (80, 81). The STIM1 SAM domain shows a very high degree of structural homology with the SAM domain of EphB2 receptor (i.e. rmsd = 2.1 Å) (Fig. 5). In general, SAM domains maintain a high degree of structural conservation despite only modest sequence identity. SAM domains are categorized as protein interaction domains; further, several modes of SAM interaction are defined from

available structural data (74, 82). For example, a constricted SAM dimer is formed via swapping of N-terminal arms with additional intermolecular contacts between the C-termini of the domain (75). Another binding mechanism involves only N-terminal arm exchange, leaving the C-termini rotated away from each other (76). A third mode occurs through hydrophobic interactions between the mid-loops (i.e. centrally located loops) and the C-terminal helices (82, 83).

The EF-hand-SAM domain intramolecular interaction

While the separately observed SAM and EF-hand domain tertiary folds within the EF-SAM structure are characteristic of many known structures in nature (Fig. 5), the intimate intramolecular association between the domains is distinctive. The significance of this interaction is underscored by the facts that the STIM1 EF-hand pair remains in an unfolded state when expressed in the absence of the SAM domain, while the instability of the SAM domain in isolation precludes any experimental work. Conversely, when the domains are expressed in tandem as per in STIM proteins, a stable and compact globular fold is realized (57, 69). The mutual folding and stability observed for Ca^{2+} -loaded EF-SAM is a result of robust hydrophobic contacts between the EF-hand pair and residues primarily from the non-polar residues opposite to the SAM bundle core. Prominent Leu195 and Leu199 side chains of $\alpha 10$ restrain the SAM domain via intimate contacts with a hydrophobic cleft shaped by several residues of the EF-hand domain (Fig. 4). The cleft residues minimally include Val68, Ile71, His72, Leu74, Met75, Leu92, Leu96, Lys104, Phe108, Ile115, and Leu120, contributed from each component of the

EF-hand not directly involved in liganding of Ca^{2+} (i.e. $\alpha 1-\alpha 2-\alpha 3-\beta 2-\alpha 4$) (Fig. 4).

Remarkably, the orientation of the anchor residues within the $\alpha 10$ helix of the SAM domain is analogous to CaM recognition of target peptides, such as smooth muscle myosin light chain kinase (smMLCK) (30, 84, 85). In the CaM intermolecular target recognition of the smMLCK peptide, the 'open' conformation of the EF-hand domains induced by Ca^{2+} binding exposes a non-polar cleft, which interacts with a hydrophobic anchor side chain (i.e. Leu813) (30, 85) on the peptide. In the STIM1 EF-hand intramolecular recognition of SAM, the 'open' conformation induced by Ca^{2+} binding forms a non-polar cleft that interacts with anchor side chains (i.e. Leu195 and Leu199) from the SAM domain. Hence, both ER luminal (i.e. STIM1) and cytosolic sensors (i.e. CaM) have evolved a Ca^{2+} -induced biomolecular interaction mediated by the 'open' conformation of integral EF-hand domains. However, the regulatory statuses are contrary to one another, with CaM in an activation conformation and STIM1 maintaining an inactivation mode (Fig. 1).

The oligomerization function of STIMs

EF-SAM intermolecular interactions

STIM1 signals opening of CRAC channels in the Ca^{2+} -depleted state, with homotypic oligomerization as a key initiation event in this activation. EF-SAM is capable of reversibly undergoing a Ca^{2+} -depletion-dependent monomer-to-oligomer transition, implying a fundamental role for this STIM region in signaling of SOCE/CRAC entry. Oligomerization of EF-SAM is coupled with destabilization and partial unfolding of the entity (57, 68). The conformational alteration (i.e. loss in secondary and change in tertiary structure) proceeds through both domains and ultimately augments the surface exposed hydrophobicity, as evidenced by far and near-UV CD data as well as thermodynamic folding analyses. The obligatory co-stabilization of the EF-hand and SAM domains in the Ca^{2+} -loaded state, the instability of the isolated domains irrespective of Ca^{2+} levels, and the destabilization-coupled oligomerization suggest that the intimate intramolecular association of the structural domains within EF-SAM is central to the sensory function of STIM proteins; thus, disruption of the EF-hand-SAM domain contacts should drive the EF-SAM initiated activation of SOCE/CRAC entry. Indeed, substitution of hydrophobic cleft residues or non-polar SAM anchor residues with charged side chains (i.e. Phe108Asp/Gly110Asp and Leu195Arg EF-SAM mutants) induces oligomerization of STIM1 EF-SAM. The mutant EF-SAM is structurally similar to Ca^{2+} -depleted wildtype EF-SAM, as assessed by electron

microscopy, far-UV CD, and SEC (i.e. amorphously oligomerized and partially unfolded). Furthermore, incorporation of these mutations into full-length STIM1 and expression in mammalian cells results in Ca^{2+} -independent and persistent SOCE/CRAC entry assessed by STIM localization and cytosolic Ca^{2+} studies (69).

Acquiring atomic resolution data of apo EF-SAM is challenging due to the polydispersity of the oligomers as well as the partially unfolded nature of the coupled subunits. However, the domains that constitute EF-SAM have been well studied in other proteins and can provide insight regarding the oligomerization mechanism of EF-SAM. A structure-based sequence alignment of several homologous SAM domains including STIM1 shows the conservation of non-polar residues in the N-terminal, mid-loop, as well as C-terminal regions (69); these components of SAM are implicated in intermolecular SAM domain interactions (74, 82) (vide infra). Mutations rationalized from these alignments that are intended to inhibit homotypic interactions are ineffective at quelling EF-SAM oligomerization, despite success in other SAM domains. For example, variants of the centrally located SAM loop either form oligomers constitutively (i.e. Leu167Arg and Thr172Arg) or have no effect on wildtype-like EF-SAM oligomerization function (i.e. Ala163Arg and Leu179Arg). Similarly, SAM N-terminal helix mutations within EF-SAM have no effect on Ca^{2+} -depletion-dependent oligomerization (i.e. Trp132Arg), while mutations in the C-terminal helix cause Ca^{2+} -insensitive oligomerization (i.e. Leu195Arg). The mutations substitute a charged cationic residue for a hydrophobic one to disrupt hydrophobicity-mediated associations. However, the magnitude of disruption by a single Arg may be insufficient to inhibit EF-SAM oligomerization, and further work is required to totally rule out previous modes of SAM interaction in the intermolecular associations of EF-SAM.

The EF-hands of Ca^{2+} -depleted CaM adopt a 'closed' conformation with interhelical angles estimated at approximately 45° (80, 81). In the 'closed' conformation, the helices of CaM assume a significantly more anti-parallel orientation, burying the non-polar cleft residues in the process. As expected, surface hydrophobicity of CaM in the 'closed' state is lower than 'open' CaM (80, 81). By contrast, differences in ANS fluorescence in addition to estimates of changes in heat capacity and denaturant dependence of unfolding for Ca^{2+} -depleted EF-SAM versus holo EF-SAM imply an increase in surface hydrophobicity for apo EF-SAM (57). It follows that the exposure of non-polar residues by the EF-hand and the SAM domains to solvent is a significant force promoting

oligomerization of Ca^{2+} -depleted EF-SAM. Hence, ER luminal sensors (i.e. STIMs) structurally adopt a Ca^{2+} -depleted state, which enhances surface hydrophobicity to promote protein–protein interactions; this mechanism is opposite to cytosolic sensors (i.e. CaM), which bury non-polar residues in the Ca^{2+} -depleted state to restrain protein–protein interactions.

Isoform crosstalk between STIM isoforms

The ability of STIM1 and STIM2 to heterotypically interact was revealed several years before the link between STIM and SOCE/CRAC entry was elucidated (39). More recently, co-localization is evident in live cell fluorescence experiments, where Ca^{2+} -binding mutant STIM1 that forms puncta independent of ER luminal Ca^{2+} levels recruits wildtype STIM2 to the same junctions (66). Additionally, ER luminal Ca^{2+} depletion triggers co-clustering of both wildtype isoforms within the same puncta (62). This STIM crosstalk may provide additional regulatory control over SOCE/CRAC entry expounded by differences in Ca^{2+} sensitivity and structural response to Ca^{2+} -depletion (86).

STIM1 versus STIM2 oligomerization kinetics

EF-SAM domains are the minimally conserved ER luminal domains of STIMs within the same species and across phylogeny (86). This conservation taken together with the role of the EF-hand-SAM interaction in initializing SOCE/CRAC entry suggests that differences in the dynamics of EF-SAM oligomerization among isoforms may afford one level of regulation in STIM functional diversity. This distinction is exemplified in the differences in oligomerization kinetics between human STIM1 and STIM2 EF-SAM. In the Ca^{2+} -free context, STIM1 EF-SAM shows no time-dependent loss in structure, as the recombinant protein shows a low level of α -helicity at high and low protein concentration reflective of a persistent oligomerization-coupled destabilized state. By contrast, STIM2 EF-SAM undergoes a much slower transformation to the lower helicity-coupled oligomerized state that is apparently dependent on relative protein concentration (i.e. higher protein concentrations oligomerize faster). The discernable concentration-dependence of STIM2 but not STIM1 EF-SAM is coherent with a comparatively slower change in molecularity for STIM2. The distinction in oligomerization kinetics between STIM1 and STIM2 EF-SAM and the coupling to a loss in α -helicity concurrent with an increase in random coil structure agrees with the inherent unfolding characteristics of the recombinant domains. STIM1 EF-SAM unfolds approximately 3.5 to 4-fold faster than STIM2 EF-SAM, as assessed by urea

denaturation experiments, implying that the STIM1 isoform more readily accesses the oligomerization-coupled destabilized state than STIM2 EF-SAM. While both isoforms sample the same range of oligomer sizes, STIM2 EF-SAM has a greater tendency to form larger oligomers, indicated by higher absolute light scattering intensity at similar protein concentrations compared with STIM1 EF-SAM (86). The distinctions in EF-SAM association kinetics are preserved when assessing oligomerization from the Ca^{2+} -loaded context. Chelation of Ca^{2+} from EF-SAM readily induces oligomerization of the STIM1 form of the protein, while STIM2 EF-SAM remains much more resistant to the homotypic assembly process (86).

In-cell data comparing various kinetic aspects of STIM-mediated SOCE/CRAC entry appear somewhat puzzling (see before). For example, HEK293 cells co-expressing STIM2 with Orai1 have a smaller and slower developing CRAC current compared with cells expressing STIM1 with Orai1 (35). However, data monitoring kinetics of puncta formation in HeLa cells with respect to ER Ca^{2+} levels (i.e. as a function of time after ethylene glycol tetraacetic acid or thapsigargin treatment) suggest that oligomerization together with translocation of STIM2 occurs at higher ER luminal Ca^{2+} levels and therefore is ostensibly quicker for STIM2 versus STIM1 (62). Comparing the in-cell data to the *in vitro* EF-SAM observations is complicated, as the full-length kinetic data minimally reflect N- and C-terminal homotypic oligomerization, ER-PM translocation, or STIM–Orai assembly processes, whereas the *in vitro* EF-SAM kinetics are indicative of only the initiation stage of SOCE/CRAC entry. Nonetheless, the effect of protein concentration on oligomerization propensity along with the notable stability differences between STIM1 and STIM2 EF-SAM may have contributed to inconsistencies observed in-cell culture with the full-length isoforms. For example, STIM protein expression is routinely manipulated in-cell culture using transient, stable, and knockdown techniques; additionally, STIM2 expression constructs employ either the wildtype ER signal peptide or a STIM1-fused ER-signal, which could alter ER targeting efficiency. Furthermore, cell culture experiments are often performed at a non-specific ambient temperature. Considering that protein concentration and stability are two imperative factors that influence oligomerization of STIM2 EF-SAM, inconsistencies in the cell culture results may have originated from irregularities in these experimental variables.

Luminal STIM sequence variability and EF-SAM stability

While the EF-SAM-encoding regions of STIM proteins are highly conserved, the extraneous lumen-oriented residues

show considerable isoform-specific variability (Fig. 2A, B). For instance, *Drosophila melanogaster*, which only encodes a single STIM protein, contains 113 residues beyond EF-SAM towards the N-terminus compared with 14 for *Caenorhabditis elegans* STIM1, 35 for human STIM1, and 47 for human STIM2 (86). The effect of the additional residues on the secondary structure of EF-SAM is minimal based on differences in the far-UV CD spectra of recombinant STIM1 and STIM2 proteins that include the full complement of luminal residues compared with EF-SAM alone. In fact, the Ca²⁺-loaded proteins from the longer constructs exhibit less CD intensity on a per residue basis (i.e. mean residue ellipticity), implying a lower overall percentage of α -helicity. A similar structural transformation occurs upon Ca²⁺-depletion as observed with the EF-SAM constructs. Nonetheless, the added residues have a marked stabilizing effect on the luminal domains in both the Ca²⁺-loaded and -depleted states, increasing the melting temperatures by approximately 15 °C in each case for both isoforms (86). Unambiguous differences in stability and oligomerization propensity are observed for human STIM1 and STIM2 EF-SAM proteins (57, 68); further tweaking of EF-SAM stability conferred by extraneous ER luminal residues may contribute to differences in sensory characteristics observed between intra- and inter-species isoforms. Hence, ER Ca²⁺ sensors employ a mechanism of genetic polymorphism to modulate the sensory responses in the ER lumen induced by changes in Ca²⁺ levels.

STIM1 activation of Orai1

The minimal Orai1 activation domain within STIM1

Co-immunoprecipitation experiments either suggest a direct interaction between STIM1 and Orai1 (21, 22) or no interaction between these ER and PM situated proteins (87). These data provide support for both a Ca²⁺ influx factor model, where a diffusible component may be induced by STIM1 oligomerization (88, 89), or a conformationally coupled model, which implies that a direct association between STIM1 and Orai1 promotes a conformational change to the PM Ca²⁺ channel, ultimately activating SOCE/CRAC entry (90). Considerably more data have come to support the direct coupling model with identification of the regional sequence determinants for the heterotypic interaction within the STIM1 and Orai1 cytosolic domains. For example, Orai1 and STIM1 are co-localized at ER-PM junctions (44, 45), fluorescence resonance energy transfer (FRET) occurs between labeled STIM1 and Orai1 after store depletion (91, 92), and expression of the entire cytosolic domain of STIM1 (i.e. without the luminal

or TM region) can activate Orai1-composed CRAC channels irrespective of ER luminal Ca²⁺ levels (54, 91, 93). Furthermore, three independent investigations have bounded the minimally required cytosolic region from STIM1 for activation of Orai1-mediated SOCE/CRAC entry to residues encoded through the ERM-like region (Fig. 2A). Muik et al. (94) show that an Orai1-activating small C-terminal fragment (OASF) consisting of residues 233–450 enhances the activation of Orai1 compared with the full cytosolic region of STIM1. A CRAC activation domain (CAD) further tapers the minimum range for maximal activation to residues 342–448 (95). Finally, maximal CRAC channel activation is observed with a STIM1 Orai activating region (SOAR) construct consisting only of residues 344–442 from STIM1 (96).

STIM1 is capable of forming puncta without the presence of Orai1 on the PM; conversely, Orai1 cannot move into puncta without coupling to STIM1 (46). Deletion of the Lys-rich region from STIM1 prevents redistribution of STIM1 to ER-PM junctions; however, when this truncation mutant is co-expressed with Orai1, puncta formation can ensue in response to luminal Ca²⁺ depletion (52, 95). The C-terminal peptides provide additional data regarding these discrepancies, in that CAD and SOAR show a pervasive cytosolic distribution when expressed without Orai1 but co-localize in puncta with Orai1 when expressed with the CRAC channel component, independent of ER luminal Ca²⁺ (95, 96). The co-localization is also observed with the longer OASF peptide (94) and is indicative of an Orai1-OASF/CAD/SOAR activating interaction. Nonetheless, co-clustering of STIM1 and Orai1 is not sufficient for activation of SOCE/CRAC, as the STIM1 truncation mutant (i.e. residues 1–440) can recruit Orai1 to puncta without activating CRAC/SOCE entry (95). Similarly, STIM1 carrying Leu347Ala/Gln348Ala mutations can form puncta with Orai1 in response to luminal Ca²⁺-depletion without activating SOCE/CRAC entry, whereas SOAR Leu347Ala/Gln348Ala variants neither form puncta nor show SOCE/CRAC entry (96).

OASF/CAD/SOAR gating of Orai1

Evidence suggests that the functional Orai1 channel pore adopts a tetrameric quaternary structure (97–99). Recombinant CAD mainly populates a tetrameric state in solution (95), whereas recombinant SOAR assumes monodisperse dimeric form (96). Similarly, the OASF peptide tends to homodimerize and disruption of this interaction by deletion of residues 420–450 precludes any SOCE/CRAC activation (94). The dimeric nature of SOAR and OASF is consistent with the

minimal stoichiometric approximation of the functional CRAC channel pore that includes an Orai1 tetramer together with a STIM1 dimer (97). CAD and SOAR both specifically interact with the C-terminal domain Orai1, as mutations (i.e. Leu273-Ser) or complete truncation of this cytosolic region within Orai1 inhibits SOCE/CRAC entry (95, 96). Similarly, these Orai1 variants are resistant to clustering and activation by wildtype STIM1 (52, 91). Deletion of the entire cytosolic N-terminal portion of Orai1 inhibits activation of SOCE/CRAC entry but not co-clustering of the mutant Orai1 with wildtype STIM1 (52). Furthermore, wildtype STIM1 inefficiently activates an Orai1 variant with the majority of the N-terminal residues deleted (i.e. Δ 1–73) (52, 96), while the SOAR and CAD domains are both capable of coupling to and activating this deletion variant (95, 96). Deletion of the downstream residues toward the first transmembrane segment of Orai1 (i.e. Δ 73–84) suppresses CAD activation of SOCE/CRAC entry (95). These data imply that OASF/CAD/SOAR interacts with both the C- and N-terminal cytosolic regions of Orai1, the C-terminal region of Orai1 is requisite for co-clustering with STIM1, and wildtype STIM1 interacts with Orai1 in a more multifarious manner than the minimal Orai1-activating domains. Consistent with this notion, a Pro3Ala/Pro5Ala mutant Orai1 is inefficiently activated by wildtype STIM1; however, a Lys684Glu/Lys685Glu mutant STIM1 restores the Pro3Ala/Pro5Ala Orai1-mediated SOCE/CRAC entry, suggesting that the STIM1 Lys-rich region may communicate with the Orai1 N-terminal Pro-rich region permitting the OASF/CAD/SOAR interactions, which activate SOCE/CRAC entry (96) in addition to targeting STIM1 to ER–PM junctions (95, 100). Nonetheless, the data show that only the OASF/CAD/SOAR region of STIM1 is necessary and sufficient to recruit Orai1 to ER–PM junctions and activate SOCE/CRAC entry through direct interactions. Hence, ER Ca^{2+} sensors have highly defined regions apart from the sensory machinery (i.e. EF-SAM) that ultimately transduce Ca^{2+} signals to effector biomolecules.

A universal signaling function for STIMs

Transient receptor potential canonical channels

Considerable data show that STIM1 regulates TRP canonical (TRPC) channels (101). TRPC channels are defined as non-selective, Ca^{2+} -permeable PM channels; moreover, many TRPC members are implicated in SOCE due to a functional sensitivity to ER luminal Ca^{2+} stores (13). An association between TRPC1 and STIM1, first established in activated platelets, also implicates type II IP_3 receptors in a ternary complex;

moreover, anti-STIM1 antibody inhibits translocation of STIM1 to the PM and prevents TRPC1–STIM1 interactions (i.e. STIM1–TRPC1 puncta formation) as well as, ultimately diminishing SOCE (102). The cytosolic C-terminal domain of STIM1 is sufficient for associations with TRPC family members (i.e. TRPC1, TRPC2, and TRPC4) with the ERM-like region of STIM1 explicitly implicated in these interactions and the Lys-rich region important for gating (54). The gating is electrostatically mediated by STIM1 residues (i.e. Lys684 and Lys685) that bind to conserved negative charges in TRPC channels (100). A requirement for Orai1 in TRPC1-dependent SOCE (103) and a direct interaction between Orai and TRPC proteins (104) have also been demonstrated. Additionally, lipid raft domains are believed to facilitate the TRPC1–STIM1 assembly process by targeting Ca^{2+} -depleted STIM1 to ER–PM junctions (105). In stark contrast to the above observations, Dehaven *et al.* (106) refute a role for STIM1 and Orai1 in regulating TRPC channels, as co-expression of STIM1 with TRPC family members fails to enhance Ca^{2+} entry, RNAi targeted to STIM1 and Orai1 has no effect on TRPC7 activity, and disruption of lipid rafts does not disturb STIM1 localization and SOCE/CRAC entry. The reasons for these discrepancies remain unclear.

ER dynamics, arachidonic acid regulated channels, and adenylyl cyclase

STIM1 expressed in mammalian cells exhibits a diffuse and tubular distribution within the ER concurrent with replete luminal Ca^{2+} stores (16, 49, 51). The fibrillar manifestation of STIM1 is co-localized with α -tubulin (51, 107). Depolymerization of the microtubules with nocodazole also disrupts the STIM1 fibrillar morphology (51, 107); however, microtubule disruption has been shown to both inhibit the activation of SOCE/CRAC entry in cells treated with nocodazole (107) and conversely, have little effect in cells treated with nocodazole (44, 51) or taxol (108). Consistent with the latter result, knockdown of the microtubule plus-end tracking protein EB1, which interacts with STIM1 and plays a role in ER remodeling, does not modify SOCE/CRAC entry (108). Overexpression of STIM1 may contribute to the seemingly microtubule depolymerization-resistant activation of SOCE/CRAC entry (107, 109, 110). Interestingly, T-cell receptor engagement with antigen-presenting cells induces STIM1–Orai1 co-accumulation at the site of stimulation (111) and in dense structures at the opposite side of the T-cell; moreover, the dense cap-like structures are not a result of ER remodeling but are inhibited by microtubule depolymerization (i.e. treatment

with colchicine) (112). Hence, while microtubule disruption does not appear to affect the inherent STIM1–Orai1 interaction, the cytoskeleton may be important in focusing these molecular CRAC complexes at immunological synapses in T-cell activation (112).

While there is conjecture as to a role for PM STIM1 in SOCE/CRAC entry signaling (17, 38), a more explicit role for PM-situated STIM1 is defined with arachidonic acid regulated Ca^{2+} -selective (ARC) channels (41, 113). Activation of ARC channels occurs via arachidonic acid acting on the intracellular side of the PM and is mediated independent of ER luminal Ca^{2+} levels (113, 114). Inhibiting glycosylation of STIM1 attenuates ARC channel activity, likely by decreasing the surface targeting of the protein (41). Additional studies show that the ARC channel pore is composed of Orai1 as well as Orai3 subunits (115).

An additional role for Orai1 and STIM1 in the regulation of adenylyl cyclase (AC) has recently come to light (116, 117). Translocation of STIM1 to sites in close apposition to the PM is critical for ER Ca^{2+} store-dependent cyclic adenosine monophosphate (cAMP) production by AC on the PM; moreover, the STIM1 translocation occurs independent of cytosolic Ca^{2+} levels and is attenuated by STIM1 puncta inhibitors [i.e. 1-(5-chloronaphthalene-1-sulfonyl)-1H-hexahydro-1,4-diazepine and 2-aminoethoxydiphenyl borate] (116). Although co-immunoprecipitation experiments fail to confirm a physical interaction between STIM1 and AC (116), imaging data show co-localization of Orai1, STIM1, and AC on lipid rafts (117). Taken together, the heterotypic interaction data support the notion that a variety of biomolecules are present in a multi-protein complex involving STIM1 at ER–PM junctions and on the PM (47). The capacity of STIMs to regulate multiple effector proteins through a common luminal sensing mechanism and the alternative function of PM STIM1 reveals diverse molecular target regulation that is not unlike CaM.

Conclusions

Modeling STIM regulation of SOCE/CRAC entry

The current reviewed data on STIM regulatory action exposes several key steps in the activation of SOCE/CRAC entry (Fig. 6). With ER Ca^{2+} stores replete of Ca^{2+} , the conserved luminal region within STIM (i.e. EF–SAM) suppresses homotypic STIM associations directed through the cytosolic domains of the protein. The stable and compact fold of Ca^{2+} -loaded EF–SAM, promoted by intimate hydrophobic interactions between the ‘open’ EF-hand pair and SAM domain, preserves the monomeric STIM1 state. Extraneous residues within the lumi-

nal region of STIM proteins that are variable among phylogeny (i.e. proximal to EF–SAM) tweak the stability of EF–SAM in a species-specific manner. Upon Ca^{2+} depletion, EF–SAM undergoes a conformational change associated with a drastic destabilization of the region, an increase in hydrophobicity and a shift to larger quaternary structure. This EF–SAM destabilization, dimerization, and oligomerization is compatible with and re-establishes homotypic cytosolic contacts between STIM molecules, probably interceded by residues encoded through the ERM-like region. The oligomerization and subsequent translocation of STIM to ER–PM junctions occurs in a cooperative manner, where the clustered OASF/CAD/SOAR domains within STIMs recruit PM-diffusing Orai1 to the puncta through heterotypic associations with the C-terminal domain of Orai1. OASF/CAD/SOAR interactions with both the N- and C-terminal domains of Orai1 play a role in mediating the gating signal from the OASF/CAD/SOAR domains. The precise atomic EF–SAM oligomerization mechanism which triggers the downstream events of SOCE is not known; furthermore, whether a conformational change is transduced from the luminal domains to the cytoplasmic domains within STIM has yet to be determined. Additionally, the function of the most variable regions within STIM molecules in mediating homo- and heterotypic intra- as well as intermolecular interactions has not been elucidated. Atomic resolution 3D structures of STIM–STIM and Orai–STIM complexes will greatly enhance our understanding of these and other outstanding questions in the signaling of SOCE/CRAC entry.

The specialized ER Ca^{2+} sensing function of STIMs

Intracellular Ca^{2+} sensors that function in the cytoplasm and sense the Ca^{2+} signal in the range of 0.1–1 μM are well characterized (see *Paradigm of intracellular Ca^{2+} sensing* for details). By virtue of multiple functional EF-hand motifs, the cytoplasmic Ca^{2+} sensors exercise high affinity (i.e. typically sub- μM) and cooperativity in Ca^{2+} binding, functioning in essence, as a molecular switch. In the past, no ER-specific Ca^{2+} sensor protein was recognized for comparison with cytosolic sensors. STIM proteins are the first described ER-specific Ca^{2+} sensors that respond to the high Ca^{2+} concentrations of the lumen and regulate SOCE/CRAC channels; moreover, structural characteristics that enable ER Ca^{2+} sensors to achieve this essential task had been unknown until the NMR-driven structure of STIM1 EF–SAM domain was elucidated.

The 3D structure revealed a number of commonalities and differences between STIMs and well-established cytoplasmic Ca^{2+} sensor proteins such as CaM (Table 1). Similar to

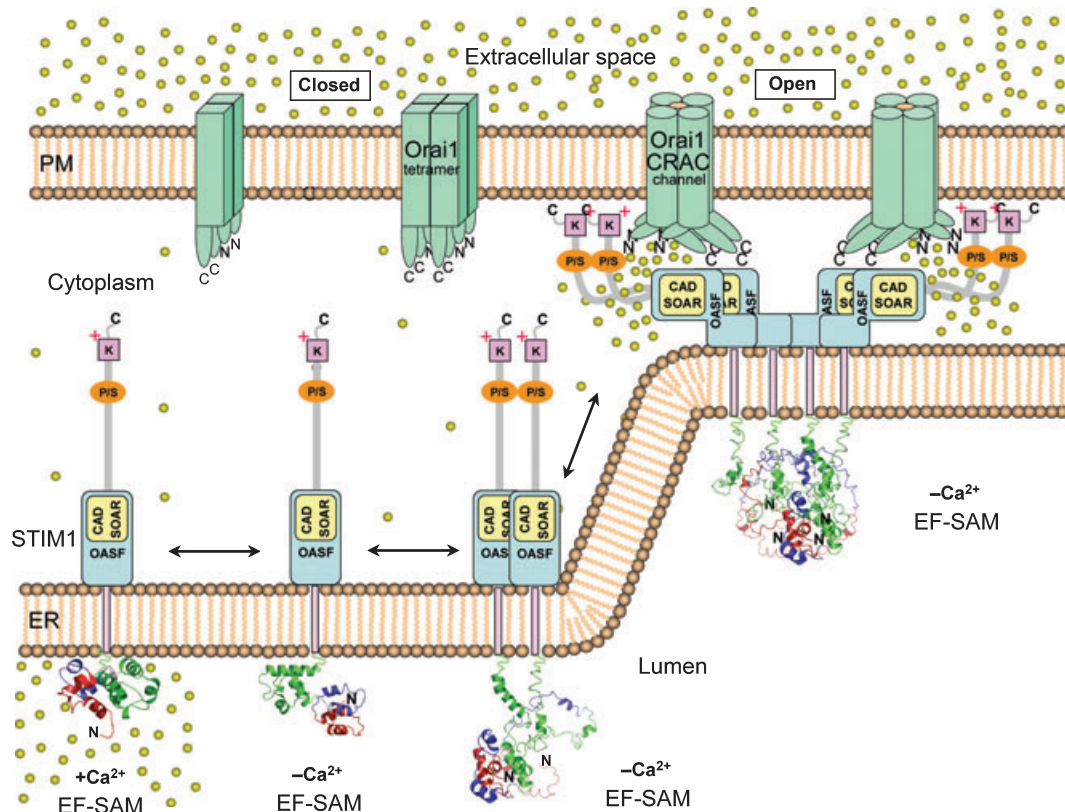


Fig. 6. Model of STIM1-mediated SOCE/CRAC activation. STIM1 EF-SAM is well-folded and stable at basally high luminal Ca^{2+} levels. Upon Ca^{2+} depletion from the ER lumen, EF-SAM becomes destabilized and transforms to a higher order structure (i.e. dimer and/or oligomer). Destabilization of EF-SAM permits and/or promotes cytosolic STIM1 association to occur and subsequent translocation of interacting STIM1 molecules to ER-PM junctions. At ER-PM junctions, the cytosolic OASF/CAD/SOAR region of STIM1 recruits and opens tetrameric Orai1 CRAC channels via interactions with the cytosolic domains of Orai1, both of which play a role in the activation of SOCE/CRAC entry. 3D structures in all figures were rendered in Pymol (120). Adapted from (69).

cytoplasmic sensors, STIM1 was discovered to possess paired EF-hand motifs. However, the paired EF-hands were unexpectedly found to intimately interact with a SAM domain, encoded in tandem to the EF-hand domain. This STIM1 luminal intramolecular interaction is mediated by a hydrophobic pocket formed by an 'open' EF-hand conformation, which is a mechanism typically employed in the target interactions of cytoplasmic Ca^{2+} sensors. Hence, the structural architecture used to facilitate both ER and cytoplasmic sensing follows a basic theme of EF-hand sensory mechanisms with a fascinating caveat: whereas 'open' EF-hand domains of cytosolic sensors are in an activated mode that promotes heterotypic effector interactions, ER Ca^{2+} sensors are dormant in the 'open' state. The inactive state of the EF-hand domains within STIM1 is preserved through intimate intramolecular interactions with the heterologous SAM domain (i.e. SAM). Intriguing distinctions extend to a few additional features. First, the second EF-hand motif in STIM1 is non-functional in Ca^{2+} binding. Disabled EF-hands are found in other members of

the CaM superfamily such as recoverin and myosin light chains, but unlike these cytosolic examples which retain multiple binding sites by virtue of encoding more EF-hand motifs (i.e. two pairs of EF-hand motifs), the single-loop binding impediment in the STIM EF-hand domain (i.e. one pair of EF-hand motifs) in combination with the SAM interaction is sufficient to generate a functionally low Ca^{2+} affinity (K_d approximately 200–600 μM) requisite for luminal Ca^{2+} sensing in the range of 200–800 μM . Moreover, the second EF-hand motif of STIM1 is essential for maintaining the overall structural architecture of the EF-SAM fold. Second, the Ca^{2+} -depleted EF-SAM domain is dramatically less stable than the Ca^{2+} loaded state. By combining a single low affinity Ca^{2+} binding site with an unprecedentedly low structural stability, ER Ca^{2+} sensors are able to homotypically oligomerize, a prerequisite to the assembly of functional SOCE/CRAC channels. Remarkably, upon ER Ca^{2+} store repletion, STIM oligomerization is completely reversible, implying that orchestrated association and dissociation occurs between luminal EF-SAM, the

Table 1. Differentiating cytosolic and ER Ca²⁺ sensors

Characteristic	Ca ²⁺ sensor	
Archetypal protein	STIM1	Calmodulin
Ca ²⁺ sensing machinery	EF-hand and SAM domains	EF-hand domains
Localization of machinery*	ER lumen	Cytosol
Number of EF-hands	1 canonical + 1 non-canonical	4 canonical
Ca ²⁺ binding stoichiometry	1	4
Ca ²⁺ binding affinity, K _d [†]	c. 200–600 μM	c. 0.1–1 μM
Hill coefficient [‡]	c. 1.5–5	c. 1.4–2
Ca ²⁺ -bound EF-hand conformation	'Open', monomer	'Open', heteromer
Ca ²⁺ -depleted EF-hand conformation	↑ Hydrophobicity, ↓ stability, ↓ α-helicity, ↑ quaternary structure	'Closed', monomer, ↓ hydrophobicity
Effector protein activation site	Cytosolic OASF/CAD/SOAR, Pro/Ser/Lys-rich regions	Cytosolic EF-hand domains
Activation mechanism	Ca ²⁺ -depletion induces: destabilization of EF SAM homotypic oligomerization translocation to puncta heterotypic protein coupling	Ca ²⁺ -loading induces: release of auto-inhibition active site remodeling heterotypic protein coupling
Origin of regulatory diversity	Genetic polymorphism, ER/PM-specific targeting, modular protein architecture	Conformational plasticity

*The sensing machinery of STIM1 is also localized in the extracellular space.

[†]The binding affinity of STIM1 EF-SAM is temperature dependent, with lower temperatures endowing a higher affinity; K_d, dissociation constant.

[‡]The coefficient >1 for STIM1 EF-SAM is indicative of the oligomerized apo state and the marked structural stabilization conferred in Ca²⁺ binding.

cytoplasmic domains, the Orai channel pore components, and other proteins associated with the SOCE/CRAC complex.

CaM employs a mechanism of conformational plasticity to modulate the action of fundamentally diverse effector proteins. STIMs also reveal an ability to universally signal several different proteins through the evolution of highly defined modular domains segregated from the sensory machinery (i.e. EF-SAM luminal sensing versus cytosolic activation domains) that ultimately transmit the luminal sensing signal to effectors. Additionally, STIMs confer a regulatory diversity by virtue of encoding multiple STIM isoforms tuned for response to spe-

cific ER luminal Ca²⁺ levels (i.e. STIM1 versus STIM2 versus *D. melanogaster* STIM).

Overall, STIM1 operates as a molecular switch in the SOCE/CRAC pathway using variable adaption of previously recognized cytosolic sensing activity, evolutionary endowed from its unique structural features. These structural characteristics define STIM proteins as ER-specific Ca²⁺ sensors that respond to the high Ca²⁺ concentrations of the lumen to regulate Orai1-composed SOCE/CRAC channels among, in all likelihood, several other ER Ca²⁺-dependent effector biomolecules.

References

- Berridge MJ, Lipp P, Bootman MD. The versatility and universality of calcium signalling. *Nat Rev Mol Cell Biol* 2000;1:11–21.
- Berridge MJ, Bootman MD, Roderick HL. Calcium signalling: dynamics, homeostasis and remodelling. *Nat Rev Mol Cell Biol* 2003;4:517–529.
- Carafoli E. The unusual history and unique properties of the calcium signal. In: Krebs J, Michalak M, eds. *CALCIUM: A Matter of Life or Death*. Amsterdam: Elsevier B.V. Publishers, 2007:3–22.
- Berridge MJ. The endoplasmic reticulum: a multifunctional signaling organelle. *Cell Calcium* 2002;32:235–249.
- Putney JW Jr. A model for receptor-regulated calcium entry. *Cell Calcium* 1986;7:1–12.
- Putney JW Jr. New molecular players in capacitative Ca²⁺ entry. *J Cell Sci* 2007;120:1959–1965.
- Le Deist F, et al. A primary T-cell immunodeficiency associated with defective trans-
- membrane calcium influx. *Blood* 1995;85:1053–1062.
- Partiseti M, Le Deist F, Hivroz C, Fischer A, Korn H, Choquet D. Defective transmembrane calcium influx demonstrated in a primary immunodeficiency by video-imaging. *C R Acad Sci III* 1994;317:167–173.
- Feske S, Prakriya M, Rao A, Lewis RS. A severe defect in CRAC Ca²⁺ channel activation and altered K⁺ channel gating in T cells from immunodeficient patients. *J Exp Med* 2005;202:651–662.

10. Feske S, et al. A mutation in Orai1 causes immune deficiency by abrogating CRAC channel function. *Nature* 2006;**441**:179–185.
11. Feske S. Calcium signalling in lymphocyte activation and disease. *Nat Rev Immunol* 2007;**7**:690–702.
12. Parekh AB, Penner R. Store depletion and calcium influx. *Physiol Rev* 1997;**77**:901–930.
13. Parekh AB, Putney JW Jr. Store-operated calcium channels. *Physiol Rev* 2005;**85**:757–810.
14. Draber P, Draberova L. Lifting the fog in store-operated Ca²⁺ entry. *Trends Immunol* 2005;**26**:621–624.
15. Roos J, et al. STIM1, an essential and conserved component of store-operated Ca²⁺ channel function. *J Cell Biol* 2005;**169**:435–445.
16. Liou J, et al. STIM is a Ca²⁺ sensor essential for Ca²⁺-store-depletion-triggered Ca²⁺ influx. *Curr Biol* 2005;**15**:1235–1241.
17. Zhang SL, et al. STIM1 is a Ca²⁺ sensor that activates CRAC channels and migrates from the Ca²⁺ store to the plasma membrane. *Nature* 2005;**437**:902–905.
18. Zhang SL, et al. Genome-wide RNAi screen of Ca(2+) influx identifies genes that regulate Ca(2+) release-activated Ca(2+) channel activity. *Proc Natl Acad Sci USA* 2006;**103**:9357–9362.
19. Vig M, et al. CRACM1 is a plasma membrane protein essential for store-operated Ca²⁺ entry. *Science* 2006;**312**:1220–1223.
20. Prakriya M, Feske S, Gwack Y, Srikanth S, Rao A, Hogan PG. Orai1 is an essential pore subunit of the CRAC channel. *Nature* 2006;**443**:230–233.
21. Vig M, et al. CRACM1 multimers form the ion-selective pore of the CRAC channel. *Curr Biol* 2006;**16**:2073–2079.
22. Yeromin AV, Zhang SL, Jiang W, Yu Y, Safrina O, Cahalan MD. Molecular identification of the CRAC channel by altered ion selectivity in a mutant of Orai. *Nature* 2006;**443**:226–229.
23. Stathopoulos PB, Ames JB, Ikura M. Structural aspects of calcium binding proteins and their interaction with targets. In: Krebs J, Michalak M, eds. *CALCIUM: A Matter of Life or Death*. Amsterdam: Elsevier B.V. Publishers, 2007:95–123.
24. Kretsinger RH, Nockolds CE. Carp muscle calcium-binding protein. II. Structure determination and general description. *J Biol Chem* 1973;**248**:3313–3326.
25. Ikura M. Calcium binding and conformational response in EF-hand proteins. *Trends Biochem Sci* 1996;**21**:14–17.
26. Lewit-Bentley A, Rety S. EF-hand calcium-binding proteins. *Curr Opin Struct Biol* 2000;**10**:637–643.
27. Nelson MR, Chazin WJ. Structures of EF-hand Ca(2+)-binding proteins: diversity in the organization, packing and response to Ca²⁺ binding. *Biometals* 1998;**11**:297–318.
28. Ikura M, Ames JB. Genetic polymorphism and protein conformational plasticity in the calmodulin superfamily: two ways to promote multifunctionality. *Proc Natl Acad Sci USA* 2006;**103**:1159–1164.
29. Linse S, Helmersson A, Forsen S. Calcium binding to calmodulin and its globular domains. *J Biol Chem* 1991;**266**:8050–8054.
30. Ikura M, Clore GM, Gronenborn AM, Zhu G, Klee CB, Bax A. Solution structure of a calmodulin-target peptide complex by multidimensional NMR. *Science* 1992;**256**:632–638.
31. Yap KL, Kim J, Truong K, Sherman M, Yuan T, Ikura M. Calmodulin target database. *J Struct Funct Genomics* 2000;**1**:8–14.
32. Klee CB, Ren H, Wang X. Regulation of the calmodulin-stimulated protein phosphatase, calcineurin. *J Biol Chem* 1998;**273**:13367–13370.
33. Michikawa T, et al. Calmodulin mediates calcium-dependent inactivation of the cerebellar type 1 inositol 1,4,5-trisphosphate receptor. *Neuron* 1999;**23**:799–808.
34. Colomer J, Means AR. Physiological roles of the Ca²⁺/CaM-dependent protein kinase cascade in health and disease. *Subcell Biochem* 2007;**45**:169–214.
35. Parvez S, et al. STIM2 protein mediates distinct store-dependent and store-independent modes of CRAC channel activation. *FASEB J* 2008;**22**:752–761.
36. Bauer MC, O'Connell D, Cahill DJ, Linse S. Calmodulin binding to the polybasic C-termini of STIM proteins involved in store-operated calcium entry. *Biochemistry* 2008;**47**:6089–6091.
37. Manji SS, et al. STIM1: a novel phosphoprotein located at the cell surface. *Biochim Biophys Acta* 2000;**1481**:147–155.
38. Spassova MA, Soboloff J, He LP, Xu W, Dziadek MA, Gill DL. STIM1 has a plasma membrane role in the activation of store-operated Ca(2+) channels. *Proc Natl Acad Sci USA* 2006;**103**:4040–4045.
39. Williams RT, et al. Identification and characterization of the STIM (stromal interaction molecule) gene family: coding for a novel class of transmembrane proteins. *Biochem J* 2001;**357**:673–685.
40. Cai X. Molecular evolution and functional divergence of the Ca²⁺ sensor protein in store-operated Ca²⁺ entry: stromal interaction molecule. *PLoS ONE* 2007;**2**:e609.
41. Mignen O, Thompson JL, Shuttleworth TJ. STIM1 regulates Ca²⁺ entry via arachidonate-regulated Ca²⁺-selective (ARC) channels without store depletion or translocation to the plasma membrane. *J Physiol* 2007;**579**:703–715.
42. Williams RT, Senior PV, Van Stekelenburg L, Layton JE, Smith PJ, Dziadek MA. Stromal interaction molecule 1 (STIM1), a transmembrane protein with growth suppressor activity, contains an extracellular SAM domain modified by N-linked glycosylation. *Biochim Biophys Acta* 2002;**1596**:131–137.
43. Soboloff J, Spassova MA, Dziadek MA, Gill DL. Calcium signals mediated by STIM and Orai proteins—a new paradigm in inter-organelle communication. *Biochim Biophys Acta* 2006;**1763**:1161–1168.
44. Luik RM, Wu MM, Buchanan J, Lewis RS. The elementary unit of store-operated Ca²⁺ entry: local activation of CRAC channels by STIM1 at ER-plasma membrane junctions. *J Cell Biol* 2006;**174**:815–825.
45. Wu MM, Buchanan J, Luik RM, Lewis RS. Ca²⁺ store depletion causes STIM1 to accumulate in ER regions closely associated with the plasma membrane. *J Cell Biol* 2006;**174**:803–813.
46. Xu P, Lu J, Li Z, Yu X, Chen L, Xu T. Aggregation of STIM1 underneath the plasma membrane induces clustering of Orai1. *Biochem Biophys Res Commun* 2006;**350**:969–976.
47. Varnai P, Toth B, Toth DJ, Hunyady L, Balla T. Visualization and manipulation of plasma membrane-endoplasmic reticulum contact sites indicates the presence of additional molecular components within the STIM1-Orai1 Complex. *J Biol Chem* 2007;**282**:29678–29690.
48. Soboloff J, Spassova MA, Tang XD, Hewavitharana T, Xu W, Gill DL. Orai1 and STIM1 reconstitute store-operated calcium channel function. *J Biol Chem* 2006;**281**:9.
49. Mercer JC, et al. Large store-operated calcium-selective currents due to co-expression of Orai1 or Orai2 with the intracellular calcium sensor, Stim1. *J Biol Chem* 2006;**281**:24979–24990.
50. Peinelt C, et al. Amplification of CRAC current by STIM1 and CRACM1 (Orai1). *Nat Cell Biol* 2006;**8**:771–773.
51. Baba Y, et al. Coupling of STIM1 to store-operated Ca²⁺ entry through its constitutive and inducible movement in the endoplasmic reticulum. *Proc Natl Acad Sci USA* 2006;**103**:16704–16709.
52. Li Z, Lu J, Xu P, Xie X, Chen L, Xu T. Mapping the interacting domains of STIM1 and Orai1 in Ca²⁺ release-activated Ca²⁺ channel activation. *J Biol Chem* 2007;**282**:29448–29456.
53. Liou J, Fivaz M, Inoue T, Meyer T. Live-cell imaging reveals sequential oligomerization and local plasma membrane targeting of

- stromal interaction molecule 1 after Ca^{2+} store depletion. *Proc Natl Acad Sci USA* 2007;**104**:9301–9306.
54. Huang GN, et al. STIM1 carboxyl-terminus activates native SOC, I(crac) and TRPC1 channels. *Nat Cell Biol* 2006;**8**:1003–1010.
 55. Luik RM, Wang B, Prakriya M, Wu MM, Lewis RS. Oligomerization of STIM1 couples ER calcium depletion to CRAC channel activation. *Nature* 2008;**454**:538–542.
 56. Strange K, Yan X, Lorin-Nebel C, Xing J. Physiological roles of STIM1 and Orai1 homologs and CRAC channels in the genetic model organism *Caenorhabditis elegans*. *Cell Calcium* 2007;**42**:193–203.
 57. Stathopoulos PB, Li GY, Plevin MJ, Ames JB, Ikura M. Stored Ca^{2+} depletion-induced oligomerization of stromal interaction molecule 1 (STIM1) via the EF-SAM region: an initiation mechanism for capacitive Ca^{2+} entry. *J Biol Chem* 2006;**281**:35855–35862.
 58. Ferrari D, et al. Endoplasmic reticulum, Bcl-2 and Ca^{2+} handling in apoptosis. *Cell Calcium* 2002;**32**:413–420.
 59. Smyth JT, Dehaven WI, Bird GS, Putney JW Jr. Ca^{2+} -store-dependent and -independent reversal of Stim1 localization and function. *J Cell Sci* 2008;**121**:762–772.
 60. Ikura M, Kay LE, Bax A. A novel approach for sequential assignment of ^1H , ^{13}C , and ^{15}N spectra of proteins: heteronuclear triple-resonance three-dimensional NMR spectroscopy. Application to calmodulin. *Biochemistry* 1990;**29**:4659–4667.
 61. Ikura M, Minowa O, Yazawa M, Yagi K, Hikichi K. Sequence-specific assignments of downfield-shifted amide proton resonances of calmodulin. *FEBS Lett* 1987;**219**:17–21.
 62. Brandman O, Liou J, Park WS, Meyer T. STIM2 is a feedback regulator that stabilizes basal cytosolic and endoplasmic reticulum Ca^{2+} levels. *Cell* 2007;**131**:1327–1339.
 63. Miranker AD, Dobson CM. Collapse and cooperativity in protein folding. *Curr Opin Struct Biol* 1996;**6**:31–42.
 64. Myers JK, Pace CN, Scholtz JM. Denaturant m values and heat capacity changes: relation to changes in accessible surface areas of protein unfolding. *Protein Sci* 1995;**4**:2138–2148.
 65. Stryer L. The interaction of a naphthalene dye with apomyoglobin and apohemoglobin. A fluorescent probe of non-polar binding sites. *J Mol Biol* 1965;**13**:482–495.
 66. Soboloff J, et al. STIM2 is an inhibitor of STIM1-mediated store-operated Ca^{2+} entry. *Curr Biol* 2006;**16**:1465–1470.
 67. Oh-Hora M, et al. Dual functions for the endoplasmic reticulum calcium sensors STIM1 and STIM2 in T cell activation and tolerance. *Nat Immunol* 2008;**9**:432–443.
 68. Zheng L, Stathopoulos PB, Li GY, Ikura M. Biophysical characterization of the EF-hand and SAM domain containing Ca^{2+} sensory region of STIM1 and STIM2. *Biochem Biophys Res Commun* 2008;**369**:240–246.
 69. Stathopoulos PB, Zheng L, Li GY, Plevin MJ, Ikura M. Structural and mechanistic insights into STIM1-mediated initiation of store-operated calcium entry. *Cell* 2008;**135**:110–122.
 70. Krebs J, Heizmann CW. Calcium-binding proteins and the EF-hand principle. In: Krebs J, Michalak M, eds. *Calcium: A Matter of Life or Death*. Amsterdam: Elsevier B.V. Publishers, 2007:51–93.
 71. Sutherland EW, Oye I, Butcher RW. The action of epinephrine and the role of the adenylyl cyclase system in hormone action. *Recent Prog Horm Res* 1965;**21**:623–646.
 72. Ebashi S, Kodama A. A new protein factor promoting aggregation of tropomyosin. *J Biochem* 1965;**58**:107–108.
 73. Ikura M, Minowa O, Hikichi K. Hydrogen bonding in the carboxyl-terminal half-fragment 78–148 of calmodulin as studied by two-dimensional nuclear magnetic resonance. *Biochemistry* 1985;**24**:4264–4269.
 74. Qiao F, Bowie JU. The many faces of SAM. *Sci STKE*. 2005;**2005**:re7.
 75. Stapleton D, Balan I, Pawson T, Sicheri F. The crystal structure of an Eph receptor SAM domain reveals a mechanism for modular dimerization. *Nat Struct Biol* 1999;**6**:44–49.
 76. Thanos CD, Goodwill KE, Bowie JU. Oligomeric structure of the human EphB2 receptor SAM domain. *Science* 1999;**283**:833–836.
 77. Green JB, Edwards TA, Trincao J, Escalante CR, Wharton RP, Aggarwal AK. Crystallization and characterization of Smaug: a novel RNA-binding motif. *Biochem Biophys Res Commun* 2002;**297**:1085–1088.
 78. Aviv T, Lin Z, Lau S, Rendl LM, Sicheri F, Smibert CA. The RNA-binding SAM domain of Smaug defines a new family of post-transcriptional regulators. *Nat Struct Biol* 2003;**10**:614–621.
 79. Barrera FN, Poveda JA, Gonzalez-Ros JM, Neira JL. Binding of the C-terminal sterile alpha motif (SAM) domain of human p73 to lipid membranes. *J Biol Chem* 2003;**278**:46878–46885.
 80. Yap KL, Ames JB, Swindells MB, Ikura M. Diversity of conformational states and changes within the EF-hand protein superfamily. *Proteins* 1999;**37**:499–507.
 81. Yap KL, Ames JB, Swindells MB, Ikura M. Vector geometry mapping. A method to characterize the conformation of helix-loop-helix calcium-binding proteins. *Methods Mol Biol* 2002;**173**:317–324.
 82. Kim CA, Bowie JU. SAM domains: uniform structure, diversity of function. *Trends Biochem Sci* 2003;**28**:625–628.
 83. Kim CA, Gingery M, Pilpa RM, Bowie JU. The SAM domain of polyhomeotic forms a helical polymer. *Nat Struct Biol* 2002;**9**:453–457.
 84. Chin D, Means AR. Calmodulin: a prototypical calcium sensor. *Trends Cell Biol* 2000;**10**:322–328.
 85. Meador WE, Means AR, Quirocho FA. Target enzyme recognition by calmodulin: 2.4 a structure of a calmodulin-peptide complex. *Science* 1992;**257**:1251–1255.
 86. Stathopoulos PB, Zheng L, Ikura M. Stromal interaction molecule (STIM) 1 and STIM2 calcium sensing regions exhibit distinct unfolding and oligomerization kinetics. *J Biol Chem* 2009;**284**:728–732.
 87. Gwack Y, et al. Biochemical and functional characterization of Orai proteins. *J Biol Chem* 2007;**282**:16232–16243.
 88. Csutora P, et al. Novel role for STIM1 as a trigger for calcium influx factor production. *J Biol Chem* 2008;**283**:14524–14531.
 89. Bolotina VM. Orai, STIM1 and iPLA2beta: a view from a different perspective. *J Physiol* 2008;**586**:3035–3042.
 90. Berridge MJ. Capacitative calcium entry. *Biochem J* 1995;**312**:1–11.
 91. Muik M, et al. Dynamic coupling of the putative coiled-coil domain of ORAI1 with STIM1 mediates ORAI1 channel activation. *J Biol Chem* 2008;**283**:8014–8022.
 92. Navarro-Borelly L, Somasundaram A, Yamashita M, Ren D, Miller RJ, Prakriya M. STIM1-Orai1 interactions and Orai1 conformational changes revealed by live-cell FRET microscopy. *J Physiol* 2008;**586**:5383–5401.
 93. Zhang SL, et al. Store-dependent and -independent modes regulating Ca^{2+} release-activated Ca^{2+} channel activity of human Orai1 and Orai3. *J Biol Chem* 2008;**283**:17662–17671.
 94. Muik M, et al. A cytosolic homomerization and a modulatory domain within STIM1 C terminus determine coupling to ORAI1 channels. *J Biol Chem* 2009;**284**:8421–8426.
 95. Park CY, et al. STIM1 clusters and activates CRAC channels via direct binding of a cytosolic domain to Orai1. *Cell* 2009;**136**:876–890.
 96. Yuan JP, Zeng W, Dorwart MR, Choi YJ, Worley PF, Muallem S. SOAR and the polybasic STIM1 domains gate and regulate Orai channels. *Nat Cell Biol* 2009;**11**:337–343.
 97. Ji W, et al. Functional stoichiometry of the unitary calcium-release-activated calcium channel. *Proc Natl Acad Sci USA* 2008;**105**:13668–13673.

98. Mignen O, Thompson JL, Shuttleworth TJ. Orai1 subunit stoichiometry of the mammalian CRAC channel pore. *J Physiol* 2008;**586**:419–425.
99. Penna A, et al. The CRAC channel consists of a tetramer formed by Stim-induced dimerization of Orai dimers. *Nature* 2008;**456**:116–120.
100. Zeng W, et al. STIM1 gates TRPC channels, but not Orai1, by electrostatic interaction. *Mol Cell* 2008;**32**:439–448.
101. Worley PF, et al. TRPC channels as STIM1-regulated store-operated channels. *Cell Calcium* 2007;**42**:205–211.
102. Lopez JJ, Salido GM, Pariente JA, Rosado JA. Interaction of STIM1 with endogenously expressed human canonical TRP1 upon depletion of intracellular Ca²⁺ stores. *J Biol Chem* 2006;**281**:28254–28264.
103. Cheng KT, Liu X, Ong HL, Ambudkar IS. Functional requirement for Orai1 in store-operated TRPC1-STIM1 channels. *J Biol Chem* 2008;**283**:12935–12940.
104. Liao Y, et al. Functional interactions among Orai1, TRPCs, and STIM1 suggest a STIM-regulated heteromeric Orai/TRPC model for SOCE/Icrac channels. *Proc Natl Acad Sci USA* 2008;**105**:2895–2900.
105. Pani B, Ong HL, Liu X, Rauser K, Ambudkar IS, Singh BB. Lipid rafts determine clustering of STIM1 in endoplasmic reticulum-plasma membrane junctions and regulation of store-operated Ca²⁺ entry (SOCE). *J Biol Chem* 2008;**283**:17333–17340.
106. Dehaven W, et al. TRPC channels function independently of STIM1 and Orai1. *J Physiol* 2009;**587**:2275–2298.
107. Smyth JT, DeHaven WI, Bird GS, Putney JW Jr. Role of the microtubule cytoskeleton in the function of the store-operated Ca²⁺ channel activator STIM1. *J Cell Sci* 2007;**120**:3762–3771.
108. Grigoriev I, et al. STIM1 is a MT-plus-end-tracking protein involved in remodeling of the ER. *Curr Biol* 2008;**18**:177–182.
109. Jermy A. STIM1 tracks growing microtubule ends. *Nat Cell Biol* 2008;**10**:384.
110. Varnai P, Hunyady L, Balla T. STIM and Orai: the long-awaited constituents of store-operated calcium entry. *Trends Pharmacol Sci* 2009;**30**:118–128.
111. Lioudyno MI, et al. Orai1 and STIM1 move to the immunological synapse and are up-regulated during T cell activation. *Proc Natl Acad Sci USA* 2008;**105**:2011–2016.
112. Barr VA, et al. Dynamic movement of the calcium sensor STIM1 and the calcium channel Orai1 in activated T-cells: puncta and distal caps. *Mol Biol Cell* 2008;**19**:2802–2817.
113. Shuttleworth TJ, Thompson JL, Mignen O. STIM1 and the noncapacitative ARC channels. *Cell Calcium* 2007;**42**:183–191.
114. Shuttleworth TJ. Arachidonic acid, ARC channels, and Orai proteins. *Cell Calcium* 2009;**45**:602–610.
115. Mignen O, Thompson JL, Shuttleworth TJ. Both Orai1 and Orai3 are essential components of the arachidonate-regulated Ca²⁺-selective (ARC) channels. *J Physiol* 2008;**586**:185–195.
116. Lefkimmatis K, Srikanthan M, Maiellaro I, Moyer MP, Curci S, Hofer AM. Store-operated cyclic AMP signalling mediated by STIM1. *Nat Cell Biol* 2009;**11**:433–442.
117. Martin AC, et al. Capacitative Ca²⁺ entry via Orai1 and stromal interacting molecule 1 (STIM1) regulates adenylyl cyclase type 8. *Mol Pharmacol* 2009;**75**:830–842.
118. Larkin MA, et al. Clustal W and Clustal X version 2.0. *Bioinformatics* 2007;**23**:2947–2948.
119. Holm L, Sander C. Dali: a network tool for protein structure comparison. *Trends Biochem Sci* 1995;**20**:478–480.
120. DeLano WL. The PyMOL Molecular Graphics System. Palo Alto, CA, USA: DeLano Scientific, 2002.